Available online at www.sciencedirect.com
SCIENCE DIRECT®
ELSEVIER
International Journal of Solids and Structures 43 (2006) 4407–4451
INTERNATIONAL JOURNAL OF SOLIDS and STRUCTURES
www.elsevier.com/locate/ijsolstr

Models of kinematics dependent anisotropic and heterogeneous friction

Alfred Zmitrowicz *

Institute of Fluid-Flow Machinery, Polish Academy of Sciences, ul.J.Fiszera 14, PL-80-952 Gdańsk, Poland

Available online 22 August 2005

Abstract

Anisotropy and heterogeneity of friction and wear can result from anisotropic roughness of engineering surfaces and from anisotropic and heterogeneous microstructures present in many materials (wood, single crystals, ceramics, composites, layer-lattice materials, polymers, biomaterials, monomolecular layers). In sliding surfaces of some materials, kinematics of sliding initiates microstructural and frictional changes. This research deals with advanced constitutive models, which describe evolutions of frictional anisotropy and heterogeneity induced by the sliding kinematics. First-, second- and higher-order constitutive equations of friction are developed with respect to powers of a sliding path curvature. The first-order equation of the friction force has two independent variables: sliding velocity unit vector and its derivative. The second- and higher-order equations are polynomials with respect to odd order tensors composed by the sliding velocity unit vector and the derivative. In the equations, friction tensors of even orders describe anisotropy and inhomogeneity of friction and effects associated with the sliding kinematics. The sliding path curvature generates: (a) an additional resistance to sliding, (b) a constraint force normal to the sliding trajectory. The friction constitutive equations satisfy the axiom of objectivity. A condition of dissipated energy restricts the friction tensors and the radius of curvature. Examples illustrate friction descriptions.

Keywords: Friction; Wear; Anisotropy; Inhomogeneity; Sliding path curvature; Friction tensors; Constitutive equations; Thermodynamic restrictions

1. Introduction

There are several physical and mechanical reasons that microstructures in bulk materials and at their surfaces undergo evolution and reorientation (e.g., from randomly to highly oriented, and from one

* Tel.: +48 58 341 12 71x134; fax: +48 58 341 61 44.
E-mail address: azmit@imp.gda.pl

0020-7683/$ - see front matter
doi:10.1016/j.ijsolstr.2005.07.001

orientation to other). During deformation in the bulk materials, the microstructure evolution is induced by the following physical phenomena: self-organization, phase transitions, formation of dislocation structures. During friction and abrasion of solid bodies, besides evolving surface roughness, changes are observed in microstructure of the sliding surfaces. The reorientation of the microstructure at the sliding surface is affected by the self-organization phenomenon, plastic flow and other structural changes in the surface and near-surface material. These physical and mechanical phenomena lead to the evolution of tribological properties at the contact interface. They may reduce (or increase) friction and wear of materials.

With the aid of pin-on-disc sliding tests, Briscoe and Stolarski (1979, 1981, 1985, 1991) observed essential changes in wear and friction for some polymeric pins taking into account various curvatures of circular sliding trajectories. This example illustrates the kinematics-dependent friction. Furthermore, kinematics of sliding can initiate microstructural and frictional changes in the sliding surfaces of layer-lattice materials as graphite and molybdenum disulphide, in polycrystalline and single-crystal beryllium and in polycrystalline magnesium. The microstructure of the sliding surfaces reorients themselves, e.g., in the direction of sliding. Privileged sliding directions (trajectories) can have complex shapes in these cases.

Modern technology stimulates developments of more credible and precise theoretical models of the frictional and wear behaviour that can cover a wide range of materials and sliding conditions. Furthermore, mathematical models of friction and wear are needed in contemporary computational mechanics and numerical software. Constructing more realistic models of friction there is required a consideration of the following influential effects: (a) anisotropy, (b) heterogeneity, (c) the kinematics of sliding, i.e., the sliding path curvature.

Different trials on the modelling of anisotropic phenomena of friction, wear and frictional heat are presented in the literature. Some theoretical models of anisotropic friction and wear are based on phenomenological postulates that are generalizations of commonly observed effects, see Zhivov (1965), Aleksandrovich et al. (1983), Hornbogen (1986), Cyfka and Hornbogen (1986), Moreau (1988), Alart (1992), Dmitriev (1993, 2002), Laursen (2002) and Mesfar et al. (2003). There have been attempts to derive equations of anisotropic friction exploiting a scheme of formulation of constitutive relations in the theory of elasto-plasticity. Some potentials were postulated whose derivatives defined friction and sliding. Such trials have been undertaken by Michałowski and Mróz (1978), Mróz and Stupkiewicz (1994), Mróz (2002), Wriggers (2002) and Hjiaj et al. (2004). Internal state variables are often used in thermodynamical theories of materials. They are parameters describing changes in the microstructure of materials during deformations. Two authors have extended this approach into anisotropic tribological phenomena, see He and Curnier (1993) and Curnier (1996). In this case, two structural tensors (material tensors) have been used as additional independent variables in the anisotropic friction equations. Therefore, the anisotropic friction models can be grouped together as follows: (a) models based on phenomenological considerations, (b) models postulated the analogy between friction and elasto-plasticity, (c) models based upon internal state variables.

The objective of this study is to model the kinematics dependent frictional anisotropy and non-homogeneity in materials and to develop advanced constitutive relations for anisotropic non-homogeneous friction. In these models, first-, second- and higher-order descriptions are considered with respect to the sliding path curvature. The friction constitutive equations are in conformity with the objectivity axiom. Restrictions on the friction constitutive relations are imposed by the second law of thermodynamics (an entropy production inequality). The subject of the study is illustrated by two examples: (a) when the friction properties (in geometrical terms) form concentric circles in the surface, (b) when the friction properties form Archimedes spirals in the surface. First trials to describe anisotropic friction with sliding path curvature effects have been undertaken in our previous studies, see Zmitrowicz (1998, 1999a,b, 2004).

2. Nature of anisotropic and heterogeneous friction and wear

The anisotropic friction is one whose properties vary with direction of sliding. The heterogeneous friction has properties that vary from point-to-point through the sliding surface. The anisotropic heterogeneous friction at a given contact point is dependent on the sliding direction and on the location of the point within the sliding area.

From the physical point of view, anisotropy of friction and wear can result from the roughness anisotropy of contacting surfaces and from anisotropy and heterogeneity present in many materials due to their particular structure. Anisotropic and non-homogeneous phenomena of friction, wear and frictional heat take place in the contact area of every rubbing pair built up by materials with heterogeneous, multiphase or anisotropic microstructure. The degree of anisotropy and inhomogeneity varies for different materials. Notice that there are two main reasons of friction heterogeneity: (a) evolving sliding surface microstructure induced by the kinematics of sliding, (b) non-homogeneity present in the surface of materials with a complex microstructure (the surface can have a mosaic structure, since different components are exposed at different points on the surface).

Short reviews of the literature devoted to experimental investigations of anisotropic friction and wear have been given in our previous papers (see Zmitrowicz, 1989, 1992a, 1993, 1995, 1999a). The present chapter of the study is concerned with several historical remarks and with a review of recently published experimental results. Friction anisotropy effects are shown in relations to particular materials and properties at their surfaces. Both types of anisotropic friction, i.e., independent and dependent on the kinematics, are reviewed in the chapter.

2.1. Early experimental measurements

Experimental measurements of friction anisotropy have a very long history. At first the anisotropic nature of hardness was discovered. Anisotropic friction and wear of various materials correspond to the anisotropic hardness. Huygens (1690) was the first who investigated the anisotropic hardness of the Iceland spar (i.e., transparent crystals of calcite). With the aid of a knife scraping along the crystal natural surfaces, he observed different resistances to scraping and polishing in different directions. A higher resistance to scraping was in the direction of the higher hardness. This way Huygens recognized main crystallographic directions of the crystals.

Exner (1873) measured the hardness anisotropy on crystal surfaces for 17th various minerals (rock-salt, fluorite, silvan, sphalerite, alum, barite, calcite, mica, gypsum and other). He observed: (a) different hardness for various crystals, (b) different hardness on various surfaces of the given crystal, (c) different hardness in various directions on the given crystal surface. In some cases, Exner observed differences in the hardness in the given direction depending on the sign of the direction (positive and negative directions).

Coulomb, Morin and Conti were the first who investigated the friction anisotropy in wood taking into account an orientation of the sliding direction with respect to wood fibers. Wood is the strongly anisotropic material, and its fibers are spread along straight or curved lines. Its physical properties vary along the following principal anisotropy axes: radial and tangential with respect to annual growth rings, longitudinal and transverse relative to the fibers, see Fig. 1. The earliest extensive investigations of the friction of wood were promoted by applications in various branches of ancient engineering and technology, e.g., in mechanical, naval and vehicle engineering. Wood was the most used material in the construction of machines in the past; iron was utilized for reinforcement or for resisting wear.

Coulomb (1785) studied the friction of sliding between two pieces of seasoned wood (oak on oak; oak on pine; pine on pine; elm on elm) and between wood and metals with or without lubricating coatings. The wood samples slid in the given direction in two different manners: (a) wood fibers were parallel in both specimens, (b) wood fibers were transversal in one specimen with respect to other. Coulomb concluded that

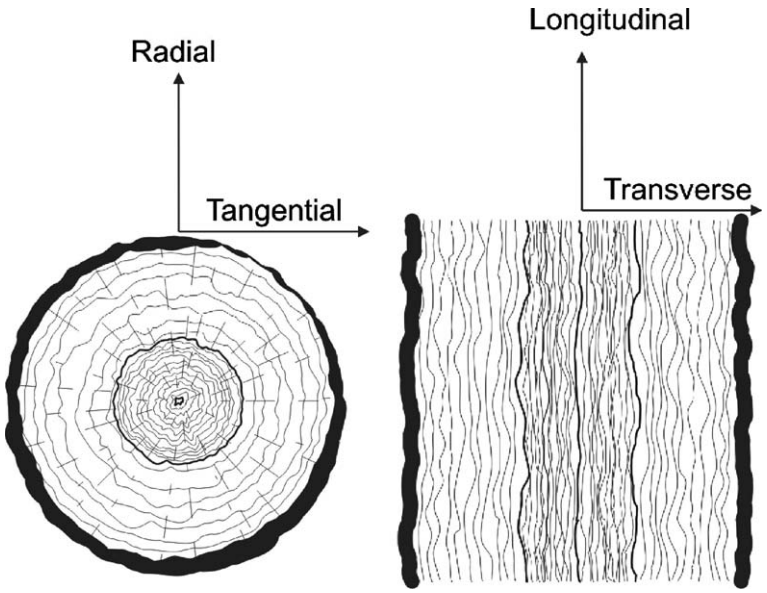

Fig. 1. Principal directions of anisotropy specified in wood.

heterogeneous surfaces, such as wood, provide different friction results in comparison with homogeneous surfaces, such as metals.

Morin (1832, 1834, 1835) investigated the friction parallel and transversal to the wood fibers in the following sorts of wood: oak on oak; oak on elm; ash-tree, pine, beech, sorb, wild pear and hornbeam on oak; and between wood and metals. Conti (1875a,b) measured the kinetic friction of wood and other materials. The specimens were allowing to slide down a very large inclined plane. Measurements of friction in wood were carried out in oak, elm, poplar—parallel and transversal to the fibers—sliding against the cast iron.

The friction coefficients measured by Coulomb were tabulated and incorporated into 19th century handbooks of engineering by Eytelwein (1808) and Gerstner von (1831). Tables of values of Morin's friction coefficients were published in his mechanics handbooks (Morin, 1843, 1846) known also from 19th century translations into German (Morin, 1844) and into Polish (Morin, 1858, 1859). In English, tables having a summary of Morin's friction experiments were published by Lanza (1901). Effects of friction anisotropy in wood are marked in all these tables. von Mises (1901–1908) in a review study cited the anisotropic friction coefficients of wood from investigations of Coulomb, Morin and Conti.

Recently Guan et al. (1983), Tong et al. (1998), Vaz and Fortes (1998) and Ohtani et al. (2003) investigated anisotropic friction and wear of the following sorts of wood: common Swedish wood (pine, spruce, oak), cork, bamboo and Katsura wood during rubbing with steel, glass, grey iron, abrasive paper and wood. In these recent experiments, the friction anisotropy in wood has been a more or less testified.

2.2. Rough engineering surfaces

Most engineering surfaces are rough and friction is known to be very sensitive to surface roughness. The directionality in friction is sometimes observed on rough surfaces where "interlocking" surface asperities lead to anisotropy effects. In general, the dependence of friction on the sliding direction arises from the specific surface roughness.

An anisotropic surface roughness is a structure in which highs and hollows in the surface are clearly oriented. Most machined surfaces of materials (i.e., surfaces obtained by cutting, grinding, finishing, super-finishing, etc.) have a definite surface roughness pattern (texture) unique to a type of machining operation. For example, there are: longitudinally oriented pattern, transversely oriented roughness pattern, oblique roughness pattern forming an inclined angle with respect to the sliding direction, circular relative to the center of the surface, radial relative to the center of the surface, etc. The surface pattern produced by machining or grinding may be modelled, to a some approximation, by a number of basic geometrical features such as straight lines, circles (including secants), polygons, curves, spirals, etc. Notice that in the case of the complex geometry of machining marks in the surface, the anisotropic friction depends on the sliding trajectory. An isotropic surface topography consists of a system of asperities without any specified orientation.

Rough surfaces of metals, polymers and other materials were investigated in the subject literature. Differences in friction coefficients were observed for the sliding parallel and perpendicular to the machining marks. Chvedov et al. (2003) attributed frictional anisotropy of a rolled aluminum sheet to the anisotropic surface topography. Anisotropic wear related to the anisotropic surface roughness was experimentally observed by Horng et al. (1994), Wang et al. (1997), Tarasov (1999a,b), Dizdar (2000) and Franklin (2001). The results show that surfaces with the transversely oriented pattern relative to the direction of sliding cause more initial surface damage than surfaces with the longitudinally oriented texture. However, the transversely oriented pattern can be helpful in lubricated contacts (e.g., in sliding bearings, in drawing processes), see Horng et al. (1994), Dizdar (2000) and Chvedov et al. (2003).

Schouterden and Lairson (1999) investigated anisotropy in friction and wear of amorphous carbon thin coatings on surfaces for hard disc applications. Friction and wear in the directions parallel and perpendicular to wear tracks were compared. Observed anisotropy effects were induced by the anisotropic topography of the wear tracks.

In environmental and geophysical large-scale observations, natural surfaces such as glacier beds are rough surfaces. Furthermore, bed topographies of the glaciers are anisotropic. This means that the bed has definite topographical irregularities. They can be treated like systems of hills and valleys in the macroscale. The glaciers slide and rub at their rough beds. Various laws of anisotropic friction and anisotropic sliding of the glaciers were studied in some papers, see Zmitrowicz (2003).

2.3. Single crystals of materials

Anisotropy is an intrinsic property of all crystalline solids. A type of atoms and an arrangement of these atoms in various directions in a crystal lattice contribute to the anisotropy effects. Therefore, physical, chemical and mechanical properties vary in different crystallographic planes and directions. Anisotropic friction, wear and hardness in crystals can be of two kinds. First, there is the variation in friction and wear when the sliding surface is changed from one crystal plane to another. Secondly, there is the variation in friction and wear when the sliding direction is changed on the given crystal plane (Bhushan, 1995).

Bowden and Tabor (1956, 1958, 1964) and Tolansky (1960) reported early experimental studies devoted to the anisotropic friction and the directional abrasion resistance on faces of diamonds. The coefficient of friction of diamond on diamond is strongly dependent on the sliding direction, varying by up to a factor of three on some crystal faces. Directions of the high friction are also the directions of the easy abrasion and polishing of the diamond. In the directions of the low friction, it is difficult to abrade the diamond (Bowden and Tabor, 1958, 1964). On the given diamond plane, there are both easier and harder polishing directions, see Fig. 2. For example, in the case of the (0 0 1) face of diamond, friction anisotropy shows four-fold symmetry (Bowden and Tabor, 1956). Recent experiments on anisotropic friction and wear in diamonds were carried out by Brookes et al. (1995) and Grillo et al. (2000).

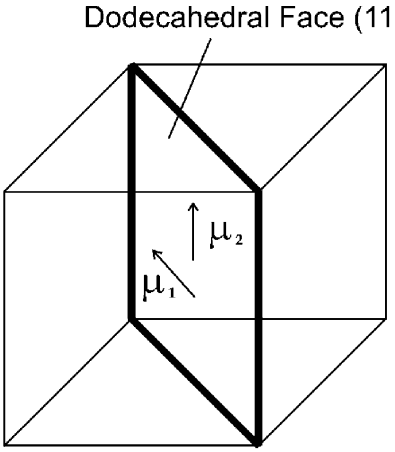

Fig. 2. Directional effects of friction and abrasion of diamond; $\mu_1 < \mu_2$, see Bowden and Tabor (1956).

Anisotropic friction between single crystal surfaces of muscovite mica have been measured by Hirano et al. (1991) and Hirano and Shinjo (1993). The changes in the frictional forces had six-fold symmetry, reflecting the hexagonal symmetry of the crystal surfaces (cleavage surfaces). Anisotropy of friction in crystals of the triglycine sulfate was investigated by Bluhm et al. (1995). Anisotropy in friction of single crystals of ice was observed by Tusima (1972). The friction coefficient was 0.034 in the prismatic plane and 0.020 in the basal plane of the ice crystal. Ko and Gellman (2000) and Gellman and Ko (2001) measured friction anisotropy between a pair of nickel single crystal surfaces Ni(1 0 0). Mancinelli and Gellman (2004) studied anisotropic friction between two Pd(1 0 0) crystal surfaces. They suggested that friction anisotropy arises from the bulk mechanical properties of the crystals.

Flom and Komanduri (2002) investigated the effect of crystal orientation and direction of sliding on friction and on wear tracks formed in single crystals under sliding a hard indenter. Anisotropy in friction and wear was observed in crystals of copper, aluminum, iron and cadmium. With the aid of wear anisotropy in single crystal alumina (sapphire), Ravikiran (2000a,b) explained wear mechanism in polycrystalline alumina, where grains were randomly oriented towards the sliding plane.

In the crystals, a bulk temperature in a large range does not change significantly anisotropy of friction. Experiments carried out by Riesz and Weber (1964) demonstrated that the orientation of clean sapphire surfaces affects friction to a considerable extent below 1300 °C. At a temperature above 1300 °C orientation effects were slight, i.e., the friction anisotropy vanished at high temperature. The melting temperature of sapphire is 2040 °C. Kanagawa et al. (2003) investigated the effect of temperature on wear for two crystal orientations of Mn–Zn ferrite. It was found that the wear rate increased with decrease of temperature in the range from −20 °C to 40 °C. The anisotropy effects are strong in low temperatures.

Scott and Wilman (1958) observed surface reorientation caused by unidirectional abrasion on surfaces of polycrystalline and single-crystal beryllium and polycrystalline magnesium. The reorientation of textures took place in a thin deformed near-surface layer. The surface subgrains had a characteristic orientation, which coincided with the abrasion direction, and it was independent on the orientation of the parent grains. This is the kinematics dependent anisotropic friction and wear.

Curved dislocation structures in the single crystals of the alloys Cu–Al were observed after plastic deformations by Prinz et al. (1981). A radius of curvature of a dislocation segment was inversely proportional to stresses (external, internal and friction stresses) acting on it. Different friction stresses were on screw and edge dislocations.

2.4. Ceramic materials

Friction, wear and hardness of ceramics are anisotropic and relate to the crystal structure (crystallographic planes and directions). Anisotropic friction and wear in silicon carbide and other materials were investigated by Buckley and Miyoshi (1984). Miyoshi and Buckley (1982) and Buckley and Miyoshi (1984) conducted experiments with silicon carbide surfaces in contact with various metals and SiC itself. An examination of wear tracts and wear debris indicated that they were influenced by the crystallographic orientation. Gatzen and Beck (2003) observed friction anisotropy in the single crystal of silicon and between two silicon surfaces. In (1 1 1) face of the silicon crystal, friction showed six-fold symmetry. In this case, the friction force varied by more than 50% depending on the sliding direction. Weick and Bhushan (2001) reviewed anisotropic friction characteristics of polycrystalline silicon used for micro-electromechanical systems.

In the growth process of the ceramic crystals, screw dislocations can be formed. Due to this, so called growth spirals are observed on the crystal faces. Tolansky (1968) studied various growth spirals on the crystal faces of the silicon carbide.

2.5. Composite materials

An addition of reinforcements (fibers, fillers, particles, whiskers, etc.) is a method for increasing the bulk mechanical/physical properties in many materials. There are three groups of microstructures of composites: group first has various randomly oriented fiber or cell arrangements, group second consists of nearly unidirectionally oriented short (discontinuous) or long (continuous) reinforcement fibers, group third is laminate. If the short fibers are in the form of non-spherical particles (e.g., plate-like), they can also be directionally oriented in the matrix.

The composites are all heterogeneous. The properties at the given point in the composite can be very different depending on whether it falls in the matrix or one of the fibers. This is because the two primary phases, fiber and matrix, have radically different properties. Most of the composites are anisotropic. It means that the physical and mechanical characteristics of the reinforced materials depend strongly on the fiber orientation, and the properties vary with the direction.

Anisotropic friction and wear of the composites were examined experimentally in numerous studies for various matrices (polymers, ceramics, glasses, light metals such as aluminum, magnesium, titanium and their alloys), and for different reinforcements (carbon or graphite, glass, silicon carbide, aluminum oxide, stainless steel, textile and polymeric fibers). Anisotropic friction and wear characteristics were reported in: (a) *metal–matrix composites* by Eliezer et al. (1978, 1979), Arikan and Murphy (1991), Nayeb-Hashemi et al. (1991), Saka et al. (1992), Belmonte et al. (1996), Sahin and Murphy (1998) and Watanabe et al. (1999); (b) *polymeric matrix composites* by Glitrow and Lancaster (1967), Tsukizoe and Ohmae (1975), Sung and Suh (1979), Chang (1983), Roberts (1985), Cyfka and Hornbogen (1986), Ciring et al. (1988), Jacobs et al. (1990), Shim and Kwon (1992), Friedrich (1993), Tripathy and Furey (1993), El-Sayed et al. (1995), El-Tayeb and Mostafa (1996), Horaguchi et al. (1996), Liang et al. (1996), Ovaert (1997), Ho and Jeng (1997), Xiao et al. (1998), Schön (2000), Franklin (2001) and Yamamoto and Hashimoto (2004); (c) *ceramic- and carbon-matrix composites* by Friedrich (1993), Liang et al. (1999a,b) and Hutton et al. (2001); (d) *glass- and rubber-matrix composites* by Minford and Prewo (1985), Wada and Uchiyama (1993), Lu et al. (1993) and Zum Gahr and Voelker (1999). It is seen that, the case of oriented "hard" fibers in "soft" polymeric matrices is of most interest from the point of view of the tribological performance.

The friction and wear of the composites are greatly influenced by the fiber orientation with respect to the sliding direction. It was found that the friction coefficients were lower when the fibers were oriented parallel rather than perpendicular to the sliding direction on composite surfaces. Furthermore, experimental results suggest, that abrasive wear properties of the composites are best when the fibers are normal to the sliding

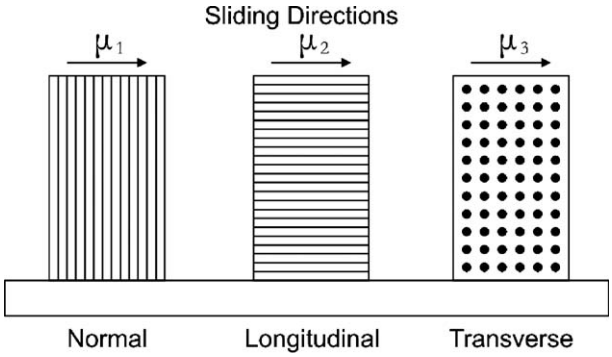

Fig. 3. Principal sliding directions in composites and friction anisotropy; $\mu_1 < \mu_2 < \mu_3$, see Sung and Suh (1979) and Tripathy and Furey (1993).

surfaces (so called ''normal orientation''). The composites exhibit the greatest wear when the fiber alignment is in the plane of contact and perpendicular to the sliding direction (''transverse orientation''), see Fig. 3. Between the two extremes in the wear resistance is the ''longitudinal orientation'', where the fiber alignment is in the contact plane and parallel to the sliding direction. Continuous, unidirectional composites show the strongest mechanical properties in the fiber direction. However, the best tribological properties of the composites in the sliding contacts would be not compatible with the best mechanical properties. When the fibers are oriented normal to the contact, then a fiber–matrix interface damage can propagate deep into the material of the composite. When the fibers lie in the plane of the sliding surface the damage propagation would be minimized.

In addition to friction and wear, the friction-generated surface temperature is an equally important parameter in technology. A dependence of the surface temperature with respect to the sliding direction was investigated in the composites by Chang (1983), Shim and Kwon (1992) and Tripathy and Furey (1993). Differences in the surface temperature or a temperature just below the sliding surface with respect to the fiber orientations in the sliding surface were found by Chang (1983) and Shim and Kwon (1992).

2.6. Layer-lattice materials

Self-lubricating layered (or lamellar) materials such as graphite and molybdenum disulphide (MoS_2) are being used to increase a service life of machine components operating in extreme conditions. Both friction and wear of the layer-lattice materials are affected considerably by the orientation, i.e., they have preferential sliding directions, see Lancaster (1966). The polycrystalline graphite is the agglomerate of monocrystals with a random orientation. When rubbed on surfaces (e.g., surfaces of metals), there is a rapid transition from the randomly oriented crystallites of graphite and molybdenum disulphide to the orientation with the crystallites nearly parallel to the sliding surface (the self-organization phenomenon), see Fig. 4. This leads to the friction coefficient evolution, and it facilitates sliding (low friction) in graphite (see Senouci et al., 1999) and in MoS_2 (see Martin et al., 1994). These are examples of the kinematics dependent anisotropic friction. Rabinowicz (1995) reported that graphite and molybdenum disulphide have low friction coefficients (about 0.1) when sliding takes place on a face parallel to the sheet direction but much higher friction coefficient (about 0.3) when sliding takes place perpendicular to the face. Notice that the graphite fibers used in the composites are strongly anisotropic; their axial and transverse mechanical and tribological properties are different, see Senouci et al. (1999).

The similar phenomenon of reorientation of particles was observed in ''wet'' contacts with molybdenum disulphide additives in lubrication oils (Persson, 2000). The MoS_2 particles consist of small flakes some

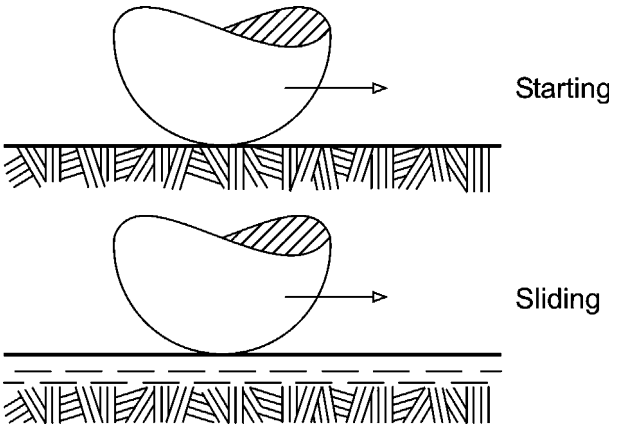

Fig. 4. The reorientation of graphite crystallites in a sliding contact (static and kinetic orientations).

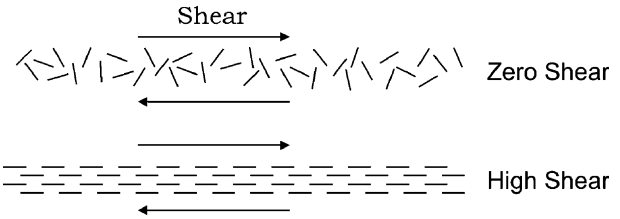

Fig. 5. The reorientation of MoS_2 flakes due to a shearing in a thin lubricant film (initial and final orientations).

thousand monolayers thick. At low shear rate, the flakes are randomly oriented, but when the shear rate increases above some critical value the flakes orient themselves in the state which corresponds to the least dissipation energy, where the crystal planes are entirely composed of streamlines of the fluid motion (Persson, 2000), see Fig. 5.

2.7. Polymers

Macromolecular polymers are repeated combinations of numerous simple chemical molecules (monomers) produced by cyclic repetition in the fabrication process. Usually, randomly distributed macromolecules do not have a specified orientation. However, sometimes the molecular chains of the polymeric materials can be aligned in one direction, so that the structure may be very highly anisotropic. In this case there is a difference in the friction for the sliding parallel and perpendicular to the chain axis. For example, the friction coefficient of PTFE was higher when the sliding occurs across the molecules than along them, see Tabor and Williams (1961) and Bowden and Tabor (1958, 1964).

Polymers undergo morphological transformations, and they transform the amorphous phase into semi-crystalline phase. For instance, the reorientation of the microstructure can take place under large deformations (or at high temperature). This leads to anisotropic properties of the polymeric material. Anisotropy of friction and wear was observed in polymeric solids by Kajiyama et al. (1996) and in polymer single crystals by Pearce and Vancso (1998).

Polytetrafluoroethylene (PTFE) and high density polyethylene (HDPE) polymers are sensitive to the orientation of their molecular chains with respect to the sliding direction. In pin-on-disc tests, Briscoe and Stolarski (1979, 1981, 1985, 1991) observed that a rate of wear of the polymers was a function of

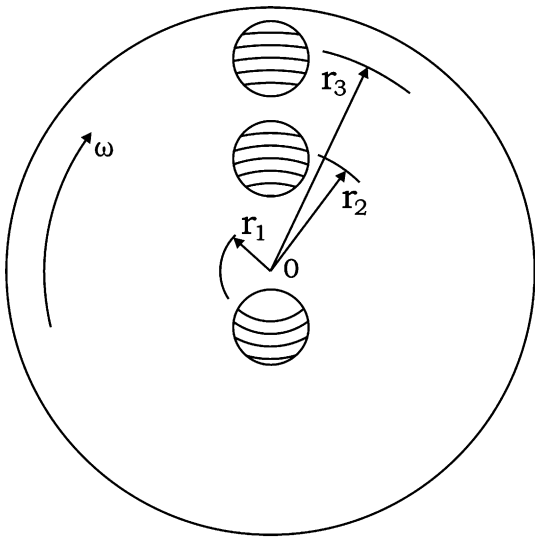

Fig. 6. Changes in wear and friction observed in some polymers for various radii of circular sliding trajectories in pin-on-disc tests, see Briscoe and Stolarski (1991).

the curvature of the circular trajectories, which the polymer pin described on the disc surface. By changing a radius of the circular path different wear rates were observed, see Fig. 6. The authors of the experiment varied the radius of rotation of the pin and the angular velocity of the disc. Therefore, the sliding conditions of the pin against the disc were maintained constant, i.e., the normal pressure and a linear sliding velocity were fixed.

In the opinion of Briscoe and Stolarski, the investigated polymers wear out by a creation of ''transferred films highly oriented'' in the direction of sliding, and the sliding occurs between oriented fibrils. Briscoe and Stolarski thought that an increase of the curvature of the sliding trajectories, and the resulting increase of reorientation of molecular chains in the contact area are responsible for the observed behaviour of the polymers. In the opinion of Briscoe and Stolarski, complex kinematics of the relative sliding between the polymer pin and the rotating disc must be taken into account. This is the example of the kinematics dependent anisotropic and heterogeneous friction and wear.

2.8. Friction asymmetry (non-centrosymmetric friction)

Some researchers refer friction asymmetry to a change in friction when the sliding direction is changed by 180°. The reversal in the direction of sliding may lead to different friction. Then, there is the different friction for sliding forward and reverse. In our nomenclature (see Zmitrowicz, 1992a,b), an anisotropic friction without central symmetry describes the variations in the friction force when changing the sliding direction by angle 180°. The simplest intuitive example is a brushed carpet having low resistance when sliding in the direction of unidirectional oriented fibers and high resistance in the opposite direction (''cat fur'' effect).

The non-centrosymmetric anisotropic friction were observed in aluminum crystals on a face with three-fold symmetry (Flom and Komanduri, 2002) and in triglycine sulfate (Bluhm et al., 1995). The friction asymmetries were found in thin monomolecular layers with the known microstructures: in Langmuir–Blodgett films on mica (Gourdon et al., 1997), in a lipid monolayer of mica (Liley et al., 1998), in polydiacetylene monolayer films (Carpick et al., 1999) and in monolayers of glycerol ester (Hisada and Knobler,

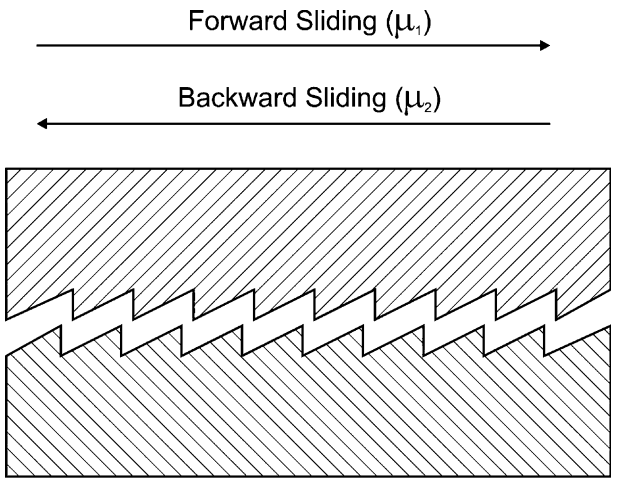

Fig. 7. The reversal in the direction of sliding leads to friction asymmetry in scale-like microstructure; $\mu_1 < \mu_2$.

2002). In experiments carried out by Kadijk and Broese van Groenou (1990), the anisotropic wear resistance changed in a video tape recorder with a head orientation and a running direction of the tape. It was noted that the reversal of the running direction of the tape leads to variations in the wear anisotropy of the manganese-zinc ferrite head of a factor 30.

Many biomaterials, e.g., all animal fibers (hair, nails, horn, hides), have very fine scale-like microstructures that cover their surfaces. The reversal in the direction of sliding leads to different friction. The friction from the tip of the scale to the root (that is against the scales) is greater than the friction from the root to the tip. The ratchet-like action of the scales induces low friction for forward motion and high friction for backward sliding (Bowden and Tabor, 1956, 1958), see Fig. 7. The friction asymmetry has been observed in snake skin specimens having the scale-like microstructure by Hazel et al. (1999); there was two-three times higher friction for the backward motion.

2.9. Friction anisotropy on micro/nano-scales

Anisotropy in friction and wear on the micro-scale is the norm. Experimental observations of anisotropic friction and wear at the atomic and nanometer scales were reported in the literature for various materials, for example: in an organic bilayer structure by Overney et al. (1994), in polymeric solids by Kajiyama et al. (1996), in crystals of molybdenum oxide sliding on molybdenum disulfide by Sheehan and Lieber (1996), in Langmuir–Blodgett films by Gourdon et al. (1997), in the lipid monolayer by Liley et al. (1998), in the snake skin by Hazel et al. (1999), in carbon thin films for hard discs by Schouterden and Lairson (1999), in glycerol ester monolayers by Hisada and Knobler (2002). Frictional anisotropy on the nano-scale has been observed at the surface of polymer single crystal by Pearce and Vancso (1998). The polymer chains within the single crystal were oriented, and the frictional anisotropy reflected this intrinsic property of the crystal. Carpick et al. (1999) examined strong friction anisotropy (300%) in monolayer films of polydiacetylenes. This effect resulted from anisotropy in mechanical properties, i.e., from an anisotropic stiffness of the film. Dickrell et al. (2005) observed that friction was a function of a nanotube orientation in films composed by multi-walled carbon nanotubes. High friction coefficient ($\mu = 0.795$) was when the nanotubes aligned normal to the contact plane and low friction coefficient ($\mu = 0.090$) when the nanotubes laid flat in the contact plane.

In the experiments, micromechanical techniques (atomic force microscopy and lateral force microscopy) were used to measure the friction forces acting between a specimen surface and a cantilever beam with a sharp contact tip at the end. Bending and torsion of the cantilever occur as a result of the contact forces at the tip. Different torsion of the cantilever during forward and reverse scanning along the same line indicates friction asymmetry (non-centrosymmetric friction), see Gourdon et al. (1997).

Molecular dynamics simulations were applied by Komanduri et al. (2000) to study the anisotropy with respect to the indentation hardness, scratch hardness and friction coefficient of aluminum single crystals. The molecular dynamics methods were used to investigate friction anisotropy in a hexagonally packed organic monolayer by Ohzono and Fujihira (2000). With the aid of the molecular dynamics, Qi et al. (2002) studied friction anisotropy between two Ni(1 0 0) surfaces.

Micro/nano friction experiments were reviewed by Weick and Bhushan (2001). There was considered the role of the crystal orientation and grain boundaries on frictional anisotropy in various crystalline materials.

3. First-order descriptions of anisotropic and heterogeneous friction

The sliding trajectory of a material point in the sliding surface in the range of time $I = (t_0, t_e)$ is described by

$$I \ni t \to \mathbf{x}(t) \in \mathscr{E}_2, \tag{1}$$

where $\mathbf{x}$ is the radius vector of the material point P with respect to the current configuration observer Oxy, t is time, $\mathscr{E}_2 = \mathscr{R} \times \mathscr{R}$ is the two-dimensional Euclidean vector space, $\mathscr{R}$ is the space of real numbers. An arc length parameter s and a one-dimensional parameterization of the plane curve (the sliding trajectory) can be introduced with the aid of the following relations:

$$s(t) = \int_{t_0}^{t} |\mathbf{V}(t)| \, \mathrm{d}\tau, \quad I \ni t \to s(t) \in \mathscr{R}. \tag{2}$$

The sliding velocity vector, its value and a unit vector tangent to the trajectory are given by

$$\mathbf{V} = \frac{\mathrm{d}\mathbf{x}}{\mathrm{d}t} = \frac{\mathrm{d}\mathbf{x}}{\mathrm{d}s}\frac{\mathrm{d}s}{\mathrm{d}t} = \mathbf{v}V, \tag{3}$$

$$V \equiv |\mathbf{V}| = \frac{\mathrm{d}s}{\mathrm{d}t}, \quad \mathbf{v} = \frac{\mathrm{d}\mathbf{x}}{\mathrm{d}s}. \tag{4}$$

According to the Frenet–Serret first formula, we have

$$\frac{\mathrm{d}\mathbf{v}}{\mathrm{d}s} = \frac{\mathbf{n}}{\rho}, \tag{5}$$

where $\mathbf{n}$ is the unit vector normal to the trajectory ($\mathbf{v} \cdot \mathbf{n} = 0$) and ρ is the sliding path curvature radius, $1/\rho$ is called the curvature, see Fig. 8.

Constitutive equations governing the phenomenon of inhomogeneous anisotropic friction we create in the frame of Amontons–Coulomb friction law. According to the phenomenological definition of dry friction as the resistance to sliding, two necessary conditions must be fulfilled: (a) contact of two solids (normal pressure), (b) sliding of one body over another (sliding velocity). That phenomenological definition focuses on commonly observed effects.

In the continuum mechanics and thermodynamics, it is customary to consider kinematical quantities as independent variables of the constitutive equations and dynamical quantities as forces, stresses, etc. as dependent ones. By the friction constitutive equation we mean a relation between the friction force vector $\mathbf{t}$ and the normal pressure N, the unit vector of the sliding velocity $\mathbf{v}$ and its derivative (5), i.e.,

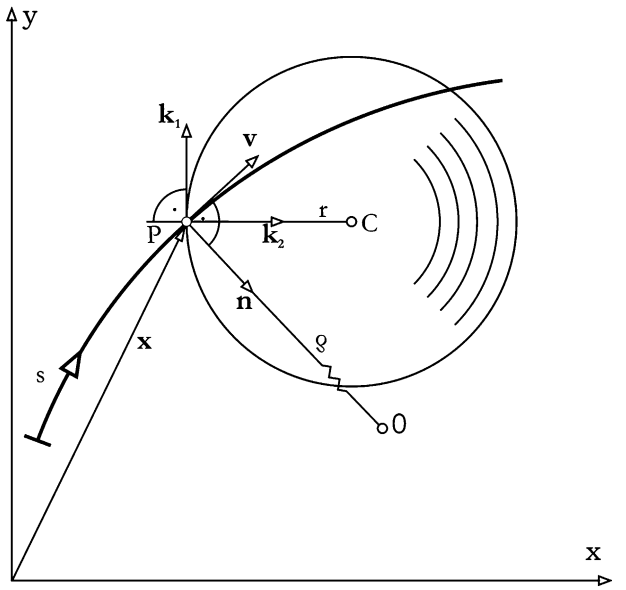

Fig. 8. The sliding trajectory of a material point in a plane with heterogeneous friction properties, which form concentric circles.

$$\mathbf{t} = \mathbf{t}\left(N, \mathbf{v}, \frac{\mathbf{n}}{\rho}\right) = -Nf\left(\mathbf{v}, \frac{\mathbf{n}}{\rho}\right), \quad f: \ \mathscr{E}_2 \times \mathscr{E}_2 \to \mathscr{E}_2. \tag{6}$$

In general, friction anisotropy refers to variations with respect to the sliding direction of the following quantities: (a) the friction coefficient, (b) the inclination angle between the friction force and the sliding direction, see Hamel (1949) and Rabinowicz (1957). The anisotropic friction coefficient μ_α and the inclination angle β of the friction force for any sliding direction can be obtained from the relations as follows:

$$\mu_\alpha = N^{-1}|\mathbf{t}|, \tag{7}$$

$$\sin\beta = \frac{\mathbf{t}\cdot\mathbf{n}}{|\mathbf{t}|}, \quad \frac{\pi}{2} \leqslant \beta \leqslant \frac{\pi}{2}. \tag{8}$$

Coefficients of the friction force components collinear with the sliding direction and normal to the sliding direction (see Fig. 9) are given by

$$\mu_\alpha^{\parallel} = -N^{-1}\mathbf{t}\cdot\mathbf{v}, \quad \mu_\alpha^{\perp} = N^{-1}\mathbf{t}\cdot\mathbf{n}. \tag{9}$$

For vanishing sliding velocity (case of sticking) the contact force is a reactive force governed by the equation of equilibrium (case of statics).

In the simples case, the friction force function (6) can be defined as a sum of two single-term polynomials, i.e.,

$$\mathbf{t} = -N\left(\mathbf{C}_1\mathbf{v} + \mathbf{E}_1\frac{\mathbf{n}}{\rho}\right), \tag{10}$$

with the following second-order friction tensors:

$$\mathbf{C}_1(\mathbf{X}) = C^{ij}\mathbf{k}_i \otimes \mathbf{k}_j, \quad i,j = 1,2, \ C^{ij} = \text{const}, \ \mathbf{k}_i = \mathbf{k}_i(\mathbf{X}), \ \mathbf{C}_1 \in \mathscr{T}_2 = \mathscr{E}_2 \otimes \mathscr{E}_2, \tag{11}$$

$$\mathbf{E}_1 = E^{kl}\mathbf{e}_k \otimes \mathbf{e}_l, \quad k,l = 1,2, \ E^{kl} \neq \text{const}, \ \{\mathbf{e}_1, \mathbf{e}_2\} \equiv \{\mathbf{v}, \mathbf{n}\}, \ \mathbf{E}_1 \in \mathscr{T}_2, \tag{12}$$

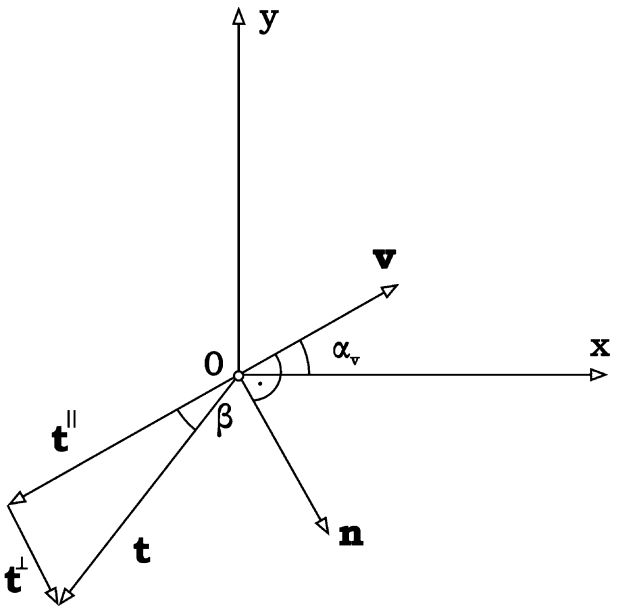

Fig. 9. The anisotropic friction force $\mathbf{t}$ acting on a material point O and its components, collinear $\mathbf{t}^{\parallel}$ and transverse $\mathbf{t}^{\perp}$ with respect to the sliding direction $\mathbf{v}$, where $\alpha_v \in \langle 0, 2\pi \rangle$ and $\beta \in \langle -\pi/2, \pi/2 \rangle$.

where $\mathscr{T}_2$ is the space being the tensor product of two vector spaces $\mathscr{E}_2$, $\{\mathbf{k}_1, \mathbf{k}_2\}$ is the basis of unit vectors adequately oriented with respect to privileged directions of inhomogeneous friction (see Fig. 8), $\mathbf{X}$ is the position vector of the material point with respect to the reference configuration observer, since any heterogeneous friction is described by a function of positions. The components E^{kl} can depend on the sliding velocity value V taken as a parameter. If the sliding path is a straight line, then the curvature vanishes ($1/\rho = 0$), and the dependence between the friction force $\mathbf{t}$ and $\mathrm{d}\mathbf{v}/\mathrm{d}s$ also vanishes. The friction equation (10) satisfies the objectivity axiom, see Zmitrowicz (1999a).

The basis $\{\mathbf{k}_1, \mathbf{k}_2\}$ can be transformed into the basis $\{\mathbf{v}, \mathbf{n}\}$ with the aid of the following rule:

$$[\mathbf{k}_1, \mathbf{k}_2]^{\mathrm{T}} = \mathbf{B}[\mathbf{v}, \mathbf{n}]^{\mathrm{T}}, \tag{13}$$

where $[\mathbf{B}] = [B_{ij}]$ $i,j = 1,2$, is a transformation matrix, $\mathbf{B} = \mathbf{B}(\mathbf{X})$. The coefficients of the transformation matrix are defined by

$$\begin{aligned} B_{11} &= \mathbf{k}_1 \cdot \mathbf{v}, \quad B_{12} = \mathbf{k}_1 \cdot \mathbf{n}, \\ B_{21} &= \mathbf{k}_2 \cdot \mathbf{v}, \quad B_{22} = \mathbf{k}_2 \cdot \mathbf{n}. \end{aligned} \tag{14}$$

Subsequent terms in the constitutive equation (10) play the following roles: $\mathbf{t}$ is the response; N, $\mathbf{v}$ and $\mathbf{n}/\rho$ are causes; $\mathbf{C}_1$ and $\mathbf{E}_1$ are parametric tensors, i.e., the tensors $\mathbf{C}_1$ and $\mathbf{E}_1$ are not arguments of the constitutive polynomial, they are coefficients of the constitutive equation. $\mathbf{C}_1$ defines frictional anisotropy and inhomogeneity at the contact. $\mathbf{E}_1$ defines effects associated with the sliding kinematics.

It is reasonable to include an analysis of symmetry properties in friction investigations. Restrictions on the friction tensor $\mathbf{C}_1$ result from the symmetry conditions. In general, the symmetry of an object is the set of all transformations of the object into itself, which leaves the object invariant. Isotropic, orthotropic, anisotropic, axi-symmetric, and uni-directional types of friction anisotropy can be distinguished with the aid of the friction tensor $\mathbf{C}_1$ and symmetry groups, see Table 1. The symmetry group $\mathscr{G}(\mathbf{C}_1)$ of the friction tensor $\mathbf{C}_1$ is a subgroup of the full orthogonal group and it satisfies the following relation:

Table 1
Linear models of anisotropic friction

Type of friction anisotropy	Symmetry elements	Restrictions on the friction tensor $\mathbf{C}_1$	Coefficients of the tensor $\mathbf{C}_1$	Restrictions on the coefficients
Isotropic	$\mathscr{O}$	$\mathbf{C}_1 = C^{11}\mathbf{1}$	$C^{11} = C^{22}$, $C^{12} = C^{21} = 0$	$C^{11} \geqslant 0$
Orthotropic	$\pm\mathbf{1}$, $\mathbf{J}_{m_1}$, $\mathbf{J}_{m_2}$	$\mathbf{C}_1 = \mathbf{C}_1^{\mathrm{T}}$	C^{11},C^{22}, $C^{12} = C^{21}$	$C^{11} \geqslant 0$, $C^{11}C^{22} - (C^{12})^2 \geqslant 0$
Anisotropic	$\pm\mathbf{1}$	None	C^{11}, C^{12}, C^{21}, C^{22}	$C^{11} \geqslant 0$, $C^{11}C^{22} - C^{12}C^{21} \geqslant 0$
Axisymmetric	$\mathbf{R}_n^{\phi}$, $\phi \in \langle 0, 2\pi\rangle$	$\mathbf{C}_1\mathbf{C}_1^{\mathrm{T}} = [(C^{11})^2 + (C^{12})^2]\mathbf{1}$	$C^{11} = C^{22}$, $C^{12} = -C^{21}$	$C^{11} \geqslant 0$, $C^{12} \in \mathscr{R}$
Unidirectional	$\pm\mathbf{1}$, $\mathbf{J}_{m_1}$, $\mathbf{J}_{m_2}$	$\det \mathbf{C}_1 = 0$	$C^{11} = C^{12} = C^{21} = C^{22}$	$C^{11} \geqslant 0$

$$\mathscr{G}(\mathbf{C}_1) = \left\{ \mathbf{R} : \mathbf{R} \in \mathscr{O}, \left(\overset{2}{\underset{1}{\otimes}} \mathbf{R} \right) \cdot \mathbf{C}_1 = \mathbf{C}_1 \right\}, \tag{15}$$

where $\mathbf{R}$ is the orthogonal tensor, $\mathscr{O}$ is the full orthogonal group and $\overset{2}{\underset{1}{\otimes}}$ denotes the following contraction:

$$\left(\overset{2}{\underset{1}{\otimes}} \mathbf{R} \right) \cdot \mathbf{C}_1 = C^{ij}\mathbf{R}\mathbf{k}_i \otimes \mathbf{R}\mathbf{k}_j. \tag{16}$$

The types of friction anisotropy described with the aid of the second-order tensor $\mathbf{C}_1$ are summarized in Table 1. There are the following elements of the symmetry groups: $+\mathbf{1}$—identity transformation, $-\mathbf{1}$—inversion, $\mathbf{J}_{m_1}$, $\mathbf{J}_{m_2}$—mirror reflections with respect to the principal directions of friction $\mathbf{m}_1$ and $\mathbf{m}_2$, $\mathbf{R}_n^{\phi}$—rotations about any axis n normal to the contact area, where ϕ is the angle of rotations. The principal directions of friction are such directions of sliding where the friction force vector $\mathbf{t}$ and the sliding velocity unit vector $\mathbf{v}$ are collinear.

Restrictions on the friction tensor coefficients shown in Table 1 follow from the second law of thermodynamics. This says that a power of the friction force is non-positive, i.e.,

$$\mathscr{P} = \mathbf{t} \cdot \mathbf{V} \leqslant 0, \quad \forall \mathbf{V} \in \mathscr{E}_2. \tag{17}$$

Let us consider the term independent on the sliding path curvature in the constitutive equation (10). After substitution of the first term in the friction equation (10) into (17), we get the restriction on the tensor $\mathbf{C}_1$, i.e.,

$$\mathbf{v}^{\mathrm{T}}\mathbf{C}_1\mathbf{v} \geqslant 0. \tag{18}$$

Hence the friction tensor $\mathbf{C}_1$ is positive-definite.

Taking the following representation of the second order tensor $\mathbf{E}_1$:

$$[\mathbf{E}_1] = \begin{pmatrix} E^{11} & E^{12} \\ E^{21} & E^{22} \end{pmatrix}, \tag{19}$$

the contraction of the tensor $\mathbf{E}_1$ and the vector of the independent variable $\mathbf{n}/\rho$ gives the following:

$$\mathbf{E}_1 \frac{\mathbf{n}}{\rho} = (E^{11}\mathbf{v} \otimes \mathbf{v} + E^{12}\mathbf{v} \otimes \mathbf{n} + E^{21}\mathbf{n} \otimes \mathbf{v} + E^{22}\mathbf{n} \otimes \mathbf{n}) \frac{\mathbf{n}}{\rho} = \frac{E^{12}}{\rho}\mathbf{v} + \frac{E^{22}}{\rho}\mathbf{n}. \tag{20}$$

Therefore, the sliding path curvature generates: (a) dissipative type component, i.e., an additional friction (E^{12}/ρ) and (b) gyroscopic type component, i.e., a sliding constraint (E^{22}/ρ).

Let us consider non-homogeneous friction properties, which form, in the contact surface: (a) concentric circles, (b) set of radii or rays emanating from the origin, see Zmitrowicz (1999a,b). Specific forms of the friction tensors are presented in Table 2. $\mathbf{k}_1$ and C^{11} are associated with the tangent to the concentric circles in the case of $\mathbf{k}_1$ and with the sliding along the circles in the case of C^{11}. $\mathbf{k}_2$ and C^{22} are defined for the sliding along the radii of the concentric circles. E^{12} is the coefficient of constraints imposed on the motion in the

Table 2
Heterogeneous anisotropic friction in the first-order description

Type of friction heterogeneity	Friction tensors $\mathbf{C}_1$, $\mathbf{E}_1$	Coefficients of the friction tensors	Restrictions on the coefficients and the radius
Concentric circles	$\mathbf{C}_1 = C^{11}\mathbf{k}_1\mathbf{k}_1 + C^{22}\mathbf{k}_2\mathbf{k}_2$	C^{11}, C^{22}	$\mathbf{v}^{\mathrm{T}}\mathbf{C}_1\mathbf{v} \geqslant 0$, $\mathbf{v}^{\mathrm{T}}\mathbf{E}_1\mathbf{n} \geqslant 0$, $\rho \in \mathscr{R}^+$ or
	$\mathbf{E}_1 = E^{12}\mathbf{v}\mathbf{n} + E^{22}\mathbf{n}\mathbf{n}$	E^{12}, E^{22}	$\mathbf{v}^{\mathrm{T}}\mathbf{C}_1\mathbf{v} > 0$, $\mathbf{v}^{\mathrm{T}}\mathbf{E}_1\mathbf{n} \leqslant 0$, $\rho \geqslant -\dfrac{\mathbf{v}^{\mathrm{T}}\mathbf{E}_1\mathbf{n}}{\mathbf{v}^{\mathrm{T}}\mathbf{C}_1\mathbf{v}}$
Rays emanating from the origin	$\mathbf{C}_1 = C^{22}\mathbf{k}_1\mathbf{k}_1 + C^{11}\mathbf{k}_2\mathbf{k}_2$ $\mathbf{E}_1$-arbitrary	C^{11}, C^{22}	$\mathbf{v}^{\mathrm{T}}\mathbf{C}_1\mathbf{v} \geqslant 0$, $\rho = \infty$

direction tangent to the sliding path, E^{22} is the coefficient of constraints imposed on the motion in the direction normal to the sliding path. The second law of thermodynamics (17) imposes restrictions on the coefficients of the friction tensors $\mathbf{C}_1$ and $\mathbf{E}_1$ and the parameter ρ, see Table 2 and Zmitrowicz (1999a).

In this particular case, the tensors $\mathbf{C}_1$ and $\mathbf{E}_1$ are defined locally, and the tensor $\mathbf{C}_1$ has orthotropic friction properties. The orthotropy group contains four symmetry elements: identity, inversion and two mirror reflections with respect to principal directions $\mathbf{k}_1$ and $\mathbf{k}_2$, i.e.,

$$\mathscr{G}(\mathbf{C}_1) = \{\pm\mathbf{1}, \mathbf{J}_{k_1}, \mathbf{J}_{k_2}\}. \tag{21}$$

The symmetry properties of the tensor $\mathbf{E}_1$ do not play an important role, and the following anisotropic symmetry can be assumed:

$$\mathscr{G}(\mathbf{E}_1) = \{\pm\mathbf{1}\}. \tag{22}$$

For $E^{22} = \text{const}$ the analyzed friction has the axial symmetry, and its group of symmetry $\mathscr{G}(\mathbf{t})$ contains rotations about the normal to the contact area crossing the center of the concentric circles C, i.e.,

$$\{\mathbf{R}_c^{\phi}\} \subset \mathscr{G}(\mathbf{t}), \quad \phi \in \langle 0, 2\pi\rangle. \tag{23}$$

The independent variable $\mathbf{n}/\rho$ of the constitutive equation depends on the position. Therefore, the analyzed friction has no symmetry with respect to translations $\delta \in \langle 0, \infty)$ along any axis

$$\{\mathbf{T}^{\delta}, \delta = 0\} \subset \mathscr{G}(\mathbf{t}), \tag{24}$$

where $\mathbf{T}^{\delta}$ is the translation vector along any axis in $\mathscr{E}_2$. Translations along arcs of the concentric circles can be introduced. These transformations are equivalent to the rotations, and they are elements of the symmetry group $\{\mathbf{R}_c^{\phi}\}$.

Let the sliding trajectory be a circle of the radius $\rho = r$ attached to the center of concentric circles, see Fig. 8. Taking the friction tensors for the concentric circles of the form presented in Table 2, we obtain from (10) the following friction force for the sliding along the concentric circles:

$$\mathbf{t} = -N\left[\left(C^{11} + \frac{E^{12}}{r}\right)\mathbf{v} + \frac{E^{22}}{r}\mathbf{n}\right]. \tag{25}$$

Then, the coefficient of the friction force component collinear with the sliding direction $\mathbf{v}$ is given by

$$\mu_{\alpha}^{\parallel}(r) = C^{11} + \frac{E^{12}}{r}, \tag{26}$$

where $C^{11} > 0$, $E^{12} \in \mathscr{R}$. We can distinguish positive and negative additional friction taking into account a sign of the coefficient E^{12}. If $E^{12} > 0$ (positive additional friction), the friction coefficient decreases when r increases. If $E^{12} < 0$ (negative additional friction), then the friction coefficient increases as r also increases.

4. Estimations of the parameters in the first-order descriptions using Briscoe and Stolarski experimental results

Friction process always involves wear of the sliding surfaces. At the macroscopic level wear is simply removal of material from the sliding solid bodies, and it can be described with the aid of a wear velocity. The wear velocity v^+ is related to a wear intensity i_A, the normal pressure N and the sliding velocity V. It can be given by the Archard law, i.e.,

$$v^+ = i_A N V. \tag{27}$$

A flux of the abraded mass m is given by

$$m = \rho_A v^+, \tag{28}$$

where ρ_A is the mass density of the wearing out body A. There are two other measures of an amount of the material loss, i.e., a depth u_n^+ of the material removed from the body in a period of the sliding time $\langle t_0, t_e\rangle \subset \mathscr{R}$ obtained by the integration of the wear velocity

$$u_n^+ = \int_{t_0}^{t_e} v^+ \,\mathrm{d}t \tag{29}$$

and a mass of the material removed from the wearing out body A given by

$$m_A = \int_S \rho_A u_n^+ \,\mathrm{d}S, \tag{30}$$

where S is the contact area of the wearing out body.

Some researchers try to define wear as a result of the yielding process of materials (Yang et al., 1993) or they made use of the fracture mechanics (Glodež et al., 1998).

The wear intensity coefficient i_A is the measure of the efficiency of material removal for the given friction force power. In general, the coefficient of the wear equation may be defined in various ways depending on the model, which is assumed. The wear equation (27) differs from the classical representation in the omission of a term representing an inverse proportionality to the surface hardness H (see Rabinowicz, 1995). In the tribology literature, the wear equation coefficient i_A used in (27) is called the dimensional wear constant or the specific wear rate. If i_A is multiplied by the hardness H, then we get the dimensionless intensity of wear $i_A H$. Therefore, the hardness H can be easily incorporated in quantitative estimates of the dimensional wear intensity coefficient i_A. One can also include anisotropy of hardness in the definition of the wear coefficient. Numerous experiments show that the surface hardness is anisotropic in many materials.

The wear intensity coefficient i_A is restricted by thermodynamic requirements as follows:

(a) *Restrictions following from the second law of thermodynamics*. An energy spent at the wear process is given by me_A, and it is positive for any sliding direction $\alpha_v \in \langle 0, 2\pi\rangle$ (see Fig. 9) and for any location of the contact point, i.e.,

$$me_A = \rho_A v^+ e_A = \rho_A i_A N V e_A \geqslant 0, \tag{31}$$

where e_A is the wear energy density (or the energy consumed by formation of a unit mass of wear debris). Taking into account that

$$\rho_A, N, V, e_A \geqslant 0, \tag{32}$$

we obtain the following restriction on the wear intensity coefficient:

$$i_A \geqslant 0. \tag{33}$$

(b) *Constraints of energy dissipated at the frictional contact*. All the energy dissipated in friction process is converted (in a priori unknown proportion) into frictional heat and the energy spent at the wear process, i.e.,

$$\mathscr{P} = \mathbf{t} \cdot \mathbf{V} = -q^{\mathrm{f}} - me_A, \tag{34}$$

where q^{f} is the component of the frictional heat flux normal to the body's boundary. Eq. (34) shows that the friction force power ($\mathscr{P}$) goes into the frictional heat flux (q^{f}) entering into the body and the energy spent on wear process of the body (me_A). Other forms of the dissipated energy are neglected. After substituting the friction force and the wear velocity, the constraint of energy dissipated (34) reduces to the following relation given in the scalar notation:

$$-(\cos\beta)\mu_\alpha NV = -q^{\mathrm{f}} - \rho_A i_A NVe_A. \tag{35}$$

Eq. (34) does not decide which part of the friction force power appears as the frictional heat and the wear process energy. Assuming that 85% of the friction power converts into frictional heat and the rest of the power transforms into wear, we get the following relation for the wear component in (35):

$$-0.15(\cos\beta)\mu_\alpha NV = -\rho_A i_A NVe_A. \tag{36}$$

Thus we have the following quantitative restriction on the wear intensity coefficient:

$$i_A = \frac{0.15}{\rho_A e_A}\mu_\alpha^{\parallel}, \tag{37}$$

since

$$\mu_\alpha \cos\beta = \mu_\alpha^{\parallel}. \tag{38}$$

It is seen from (37) that: the higher e_A, the higher wear resistance. An open question is: how to estimate the wear energy density e_A? It has a few components: (a) internal energy of the body in its natural state, (b) energy of elastic and plastic deformations, (c) stored thermal energy and other. Rabinowicz (1995, p. 162) suggested that in rough calculations of wear such as (34)–(37) one should consider the sliding body "loaded to the limit". It seems to be a right way, in trials to estimate the wear energy density. In the example calculations, we use the following average values of the friction coefficient and the wear intensity coefficient, which are typical for polymers

$$\mu_\alpha^{\parallel} = 0.18, \quad i_A = 0.5 \times 10^{-6}\ \mathrm{MPa}^{-1}. \tag{39}$$

The phenomena of abrasive wear and dry friction are usually treated as inseparable. Anisotropy of abrasion may be explained in terms of an identical anisotropy in friction, see Sung and Suh (1979) and Jacobs et al. (1990). Therefore, the coefficient of the anisotropic heterogenous friction force and the anisotropic heterogeneous wear rate can be assumed to be functions of the same type.

Let us postulate that the wear intensity coefficient $i_A(r)$ and the friction coefficient $\mu_\alpha^{\parallel}(r)$ are the functions of the same type with respect to the variable $r \in \langle 0, \infty)$. We say that a close similarity exists between the wear intensity i_A relation and the friction coefficient $\mu_\alpha^{\parallel}$ equation, i.e., both coefficients are the similar functions of the radius r. Let us denote that fact as follows:

$$i_A(r) \sim \mu_\alpha^{\parallel}(r). \tag{40}$$

The function $\mu_\alpha^{\parallel}(r)$ is given by (26), so that we have

$$i_A(r) = i_1 + \frac{\xi_1}{r}, \tag{41}$$

where i_1 and ξ_1 are constants, $i_1 > 0$, $\xi_1 \in \mathscr{R}$. In our previous study (Zmitrowicz, 1993), we assumed the similarity between the wear intensity i_A and the friction coefficient μ_α, i.e., $i_A \sim \mu_\alpha$. The similar approach we have used in the case of anisotropic frictional heat (Zmitrowicz, 1995). The actual proposition (40) is better one. In the description (41), values of radii of the circular sliding trajectories are restricted, i.e.,

$$r \geqslant -\frac{\xi_1}{i_1}, \tag{42}$$

since $i_A(r)$ is non-negative in any case, see inequality (33).

In the pin-on-disc experiments for some polymeric pins, Briscoe and Stolarski (1979, 1981, 1985) observed a maximum wear rate for the large radius of the circular sliding trajectory and a significant reduction in the rate when the radius approached the radius of the pin (see Fig. 6). Let us assume the following values of the constants in the friction and wear equations (26) and (41)

$$C^{11} = 0.15, \quad E^{12} = 0.0005 \text{ m}, \tag{43}$$

$$i_1 = 0.8 \times 10^{-6} \text{ MPa}^{-1}, \quad \xi_1 = -0.35 \times 10^{-8} \text{ MPa}^{-1} \text{ m}. \tag{44}$$

After substitution (44) into (42), we obtain the restriction for the radii of the circular trajectories, i.e., $r \geqslant 0.0044$ m. We are faced by a problem of units for E^{12} and ξ_1. They are quoted in units of m and MPa^{-1} m, respectively. Notice, there is a similarity to units of the coefficient of rolling friction. According to Coulomb model of rolling friction, the coefficient of rolling friction is measured in units of length, e.g., in m.

The following four values of the independent variable r are taken into consideration:

$$r_1 = 0.0065 \text{ m}, \quad r_2 = 0.025 \text{ m}, \quad r_3 = 0.065 \text{ m}, \quad r_4 = \infty. \tag{45}$$

Then from Eqs. (26) and (41) we get

$$\begin{aligned} &r_1 = 0.0065 \text{ m} \to \mu_\alpha^{\parallel} = 0.227, \quad i_A = 0.26 \times 10^{-6} \text{ MPa}^{-1}, \\ &r_2 = 0.025 \text{ m} \to \mu_\alpha^{\parallel} = 0.17, \quad i_A = 0.66 \times 10^{-6} \text{ MPa}^{-1}, \\ &r_3 = 0.065 \text{ m} \to \mu_\alpha^{\parallel} = 0.158, \quad i_A = 0.75 \times 10^{-6} \text{ MPa}^{-1}, \\ &r_4 = \infty \to \mu_\alpha^{\parallel} = 0.15, \quad i_A = 0.8 \times 10^{-6} \text{ MPa}^{-1}. \end{aligned} \tag{46}$$

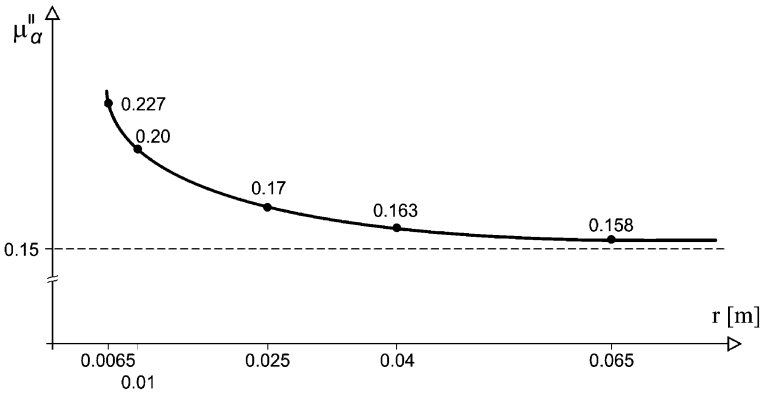

Fig. 10. Changes in the friction coefficient $\mu_\alpha^{\parallel}$ for various radii r of circular sliding trajectories. This is a comparison of the model with Briscoe and Stolarski experimental results.

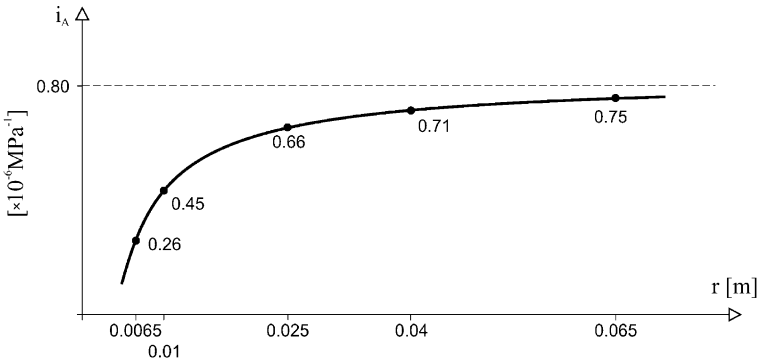

Fig. 11. Changes in the wear intensity coefficient i_A for various radii r of circular sliding trajectories (i_A is quoted in 10^{-6} MPa^{-1}). This is a comparison of the model with Briscoe and Stolarski experimental results.

Figs. 10 and 11 illustrate the evolving friction coefficient $\mu_{\alpha}^{\parallel}(r)$ and the wear intensity coefficient $i_A(r)$. The changes are induced by the sliding path curvature. These estimations coincide very well with the results of Briscoe and Stolarski (1979, 1981, 1985). The wear intensity i_A increases significantly as r also increases (a factor of about 3). A difference in the friction coefficient $\mu_{\alpha}^{\parallel}$ is smaller, and the friction decreases as r increases. In general, wear is more sensitive to any change in the contact conditions while friction varies relatively little. Additionally, these examples show an unusual behaviour of friction and wear, since the maximum wear rate i_A and the maximum friction coefficient $\mu_{\alpha}^{\parallel}$ are for different values of the radius r. Notice that in numerous examples known from the tribology literature, the maximum anisotropic wear and the maximum anisotropic friction are at the same point.

5. Friction asymmetry in the first-order descriptions

Non-centrosymmetric friction can occur in a plane with non-homogeneous friction properties which form concentric circles in the surface. In this case, there are two privileged sliding directions: along concentric circular trajectories and along radial trajectories. The friction force can depend on the sense of the sliding direction. Therefore, the sliding along concentric circular trajectories meets different friction in the clockwise direction and in the anticlockwise direction. The sliding along radii has different friction for the motion from the origin to outside and for the motion from the outside to the origin.

Anisotropic friction models described with the aid of the friction tensors $\mathbf{C}_1$ presented in Table 1 are centrosymmetric. The inversion $-\mathbf{1}$ describes anisotropy having central symmetry.

In the non-centrosymmetric case a change of sense of the sliding direction must be connected with a variation in anisotropy description. An introduction of friction tensors $\mathbf{C}_1$ with components depending on the sliding direction makes it possible. Let us assume that the friction tensor $\mathbf{C}_1$ is a function of the sliding direction parameter α_v, i.e.,

$$\mathbf{C}_1(\alpha_v, \mathbf{X}) = C^{ij}(\alpha_v)\mathbf{k}_i(\mathbf{X}) \otimes \mathbf{k}_j(\mathbf{X}), \quad \alpha_v \in \langle 0, 2\pi \rangle, \qquad i, j = 1, 2, \tag{47}$$

where α_v is the measure of an oriented angle between the unit vector $\mathbf{v}_0$ of a reference direction (e.g., Ox axis) and the sliding velocity unit vector $\mathbf{v}$, see Fig. 9. Let us consider the friction tensor $\mathbf{C}_1(\alpha_v, \mathbf{X})$ which is a trigonometrical polynomial of α_v as follows:

$$\mathbf{C}_1(\alpha_v, \mathbf{X}) = \mathbf{C}_{10}(\mathbf{X}) + \mathbf{C}_{11}(\mathbf{X}) \cos(n_1\alpha_v) + \mathbf{C}_{12}(\mathbf{X}) \sin(m_1\alpha_v), \quad n_1, m_1 = 0, 1, 2, 3, \ldots, \tag{48}$$

where $\mathbf{C}_{10}$, $\mathbf{C}_{11}$, $\mathbf{C}_{12}$ are the second-order tensors which are constants of the polynomial (48). Hence, the friction constitutive equation (6) has the following form:

$$\mathbf{t} = -N\left([\mathbf{C}_{10} + \mathbf{C}_{11}\cos(n_1\alpha_v) + \mathbf{C}_{12}\sin(m_1\alpha_v)]\mathbf{v} + \mathbf{E}_1\frac{\mathbf{n}}{\rho}\right). \tag{49}$$

The friction equation (49) satisfies the axiom of material objectivity, since the orthogonal transformations $\mathbf{R} \in \mathcal{O}$ do not change angles between two arbitrary vectors, i.e.,

$$(\mathbf{R}\mathbf{v}_0)\cdot(\mathbf{R}\mathbf{v}) = \mathbf{v}_0\cdot\mathbf{v}, \quad \forall \mathbf{v}_0, \mathbf{v} \in \mathscr{E}_2. \tag{50}$$

Therefore, the oriented angle α_v leaves unchanged after the orthogonal transformation. The restriction $\mathbf{v}^{\mathrm{T}}\mathbf{C}_1\mathbf{v} \geqslant 0$ following from the second law of thermodynamics, see (18), we extend taking into account new definition of the friction tensor $\mathbf{C}_1$, i.e.,

$$\mathbf{V}^{\mathrm{T}}[\mathbf{C}_{10} + \mathbf{C}_{11}\cos(n_1\alpha_v) + \mathbf{C}_{12}\sin(m_1\alpha_v)]\mathbf{V} \geqslant 0, \tag{51}$$

for every $\mathbf{V}$ and $\alpha_v \in \langle 0, 2\pi\rangle$.

Let us consider the friction equation (49) in the following simplified form:

$$\mathbf{t} = -N\left([\mathbf{C}_{10} + \mathbf{C}_{11}\cos(n_1\alpha_v)]\mathbf{v} + \mathbf{E}_1\frac{\mathbf{n}}{\rho}\right), \tag{52}$$

where $n_1 = 1$ and the tensors $\mathbf{C}_{10}$, $\mathbf{C}_{11}$ have the following representations:

$$[\mathbf{C}_{10}] = \begin{pmatrix} C_0^{11} & 0 \\ 0 & C_0^{22} \end{pmatrix}, \quad [\mathbf{C}_{11}] = \begin{pmatrix} C_1^{11} & 0 \\ 0 & C_1^{22} \end{pmatrix}. \tag{53}$$

Then, the friction coefficient (26) for the sliding along concentric circular trajectories of the radius r is defined as follows:

$$\mu_\alpha^{\parallel}(r) = C_0^{11} + C_1^{11}\cos\alpha_v + \frac{E^{12}}{r}. \tag{54}$$

The friction coefficient for the sliding along rectilinear radial trajectories ($\rho = \infty$) takes the form

$$\mu_\alpha^{\parallel} = \mu_\alpha = C_0^{22} + C_1^{22}\cos\alpha_v. \tag{55}$$

The status of the forward and backward sliding is distinguished by the factor α_v, i.e.,

$$\alpha_v = \begin{cases} 0 & \text{if forward sliding,} \\ \pi & \text{if backward sliding.} \end{cases} \tag{56}$$

The inversion $-\mathbf{1}$ is not the symmetry transformation in this case.

6. Compositions of two surfaces in the first-order descriptions

In the tribology literature there are trials to study changes of anisotropic friction in dependence on the compositions of the contacting surfaces. Experimental measurements of friction for various compositions of two rough surfaces with homogeneous orthotropic friction properties were carried out by Sharpin (1957). A change of frictional anisotropy with respect to different compositions of two faces of contacting diamond crystals has been observed by Seal (1957). Schön (2000) measured friction coefficients for two different combinations of flat composite specimen pairs (graphite fiber/epoxy matrix) taking different orientations of the fibers with respect to the sliding direction. Friction for various combinations of the contacting surfaces of silicon crystals was investigated by Gatzen and Beck (2003).

Let us assume that for the given normal pressure N the resultant friction force at the contact of two surfaces is equal to the product of a "composition coefficient" by the sum of the friction forces obtained for each surface taken separately

$$\mathbf{t}_{AB} = \kappa(\overset{(A)}{\mathbf{t}} + \overset{(B)}{\mathbf{t}}), \tag{57}$$

where κ is the experimental composition coefficient, $\overset{(A)}{\mathbf{t}}$ and $\overset{(B)}{\mathbf{t}}$ are friction forces which correspond to the friction when sliding a third body with isotropic homogeneous friction properties along the contacting surfaces (A) and (B). We call the relation (57) as the additive composition law. Of course, one can assume other composition laws different than Eq. (57). For example, the resultant friction force at the contact of two surfaces can be equal to a minimum of the friction forces obtained for each surface taken separately, i.e.,

$$\mathbf{t}_{AB} = \min\{\overset{(A)}{\mathbf{t}}, \overset{(B)}{\mathbf{t}}\}. \tag{58}$$

Let us compare the additive law (57) with the minimum type law in the form (58) in the case of isotropic friction. According to these laws of the composition, the resultant friction coefficients $\overset{(AB)}{\mu}$ can be calculated with the aid of the following formulae:

$$\overset{(AB)}{\mu} = \kappa(\overset{(A)}{\mu} + \overset{(B)}{\mu}), \tag{59}$$

$$\overset{(AB)}{\mu} = \min\{\overset{(A)}{\mu}, \overset{(B)}{\mu}\}. \tag{60}$$

We take into account friction coefficients for various materials measured by Bowden and Tabor (1956) and Kragelskii (1965).

First example. Measured coefficients are as follows: for steel–steel $\overset{(A)}{\mu} = 0.17$, for cast iron-cast iron $\overset{(B)}{\mu} = 0.28$ and for steel–cast iron $\overset{(AB)}{\mu} = 0.32$; the calculated friction coefficient according to Eq. (59) for steel–cast iron is given by

$$\overset{(AB)}{\mu} = 0.71(0.17 + 0.28) \approx 0.32, \tag{61}$$

where $\kappa = 0.71$. It is seen that, in the additive law, the composition coefficient κ can take various values, and the law (57) can be easily adopted to real situations.

Second example. Measured coefficients: for steel–steel $\overset{(A)}{\mu} = 0.17$, for graphite–graphite $\overset{(B)}{\mu} = 0.1$ and for steel–graphite $\overset{(AB)}{\mu} = 0.1$; the calculated coefficient according to Eq. (60) for steel–graphite is as follows:

$$\overset{(AB)}{\mu} = \min\{0.17, 0.1\} = 0.1. \tag{62}$$

The minimum type law gives correct results in this case, since the friction properties of the second material are strongly dominated. That situation is typical for the solid lubricants (graphite, PTFE, etc.). In our opinion, the minimum type law (58) is very restrictive, and it has a restricted range of applications. Therefore, we use the additive law (57).

Property 1. *The combination of the following two surfaces, the first surface with non-homogeneous friction properties in the form of concentric circles and the second surface with other friction properties, gives the resultant friction which depends on the composed friction types and on the manner of composition.*

In the first-order description, the friction forces for surfaces (A) and (B) can be represented by

$$\overset{(s)}{\mathbf{t}} = -N\left[\underset{1}{\overset{(s)}{\mathbf{C}}}\,\overset{(s)}{\mathbf{v}} + \overset{(s)}{\mathbf{E}}_1 \frac{\overset{(s)}{\mathbf{n}}}{\overset{(s)}{\rho}}\right], \quad s \equiv A, B, \tag{63}$$

where

$$\overset{(s)}{\mathbf{C}}_1 = \overset{(s)}{C}{}^{11}\ \overset{(s)}{\mathbf{k}}_1 \otimes \overset{(s)}{\mathbf{k}}_1 + \overset{(s)}{C}{}^{22}\ \overset{(s)}{\mathbf{k}}_2 \otimes \overset{(s)}{\mathbf{k}}_2, \tag{64}$$

$$\overset{(s)}{\mathbf{E}}_1 = \overset{(s)}{E}{}^{12}\ \overset{(s)}{\mathbf{v}} \otimes \overset{(s)}{\mathbf{n}} + \overset{(s)}{E}{}^{22}\ \overset{(s)}{\mathbf{n}} \otimes \overset{(s)}{\mathbf{n}}. \tag{65}$$

The sliding path is always a common curve in the surfaces (A) and (B) being in contact. An observer in the body (A) sees one sliding trajectory of the body, and an observer in the body (B) also sees one sliding path. For instance: (a) any solid body sliding down an inclined surface draws a rectilinear sliding trajectory, (b) a fixed pin pressed to the rotating disc draws the circular sliding trajectory (pin-on-disc tests), (c) the pin moving with the given velocity along a radius of the rotating disc draws a spiral trajectory. The sliding trajectory can be uniquely specified not only in the case of two contacting rigid bodies but also in the case of two deformable bodies. In every-day life, one sliding trajectory can be observed in: railway wheel rolling on a rail, automobile tire sliding against a road, shaft rotating in journal bearings, toothed gear wheels rolling and sliding one over another, rubber eraser rubbing out pencil marks on a paper, etc.

Two contacting and sliding bodies realize one relative motion, and they have at the given contact point one relative motion trajectory and one sliding path curvature. Therefore, the sliding path curvature and the friction force are uniquely determined. Hence, quantities relating to the sliding path are identical for both surfaces at the given contact point, i.e.,

$$\overset{(A)}{\rho} = \overset{(B)}{\rho} \equiv \rho, \tag{66}$$

$$\overset{(A)}{\mathbf{v}} = \overset{(B)}{\mathbf{v}} \equiv \mathbf{v}, \tag{67}$$

$$\overset{(A)}{\mathbf{n}} = \overset{(B)}{\mathbf{n}} \equiv \mathbf{n}. \tag{68}$$

These facts do not depend on the relative positions of the contacting surfaces.

The unit vectors $\{\overset{(s)}{\mathbf{k}}_1, \overset{(s)}{\mathbf{k}}_2\}$ relating to the physical properties of the surfaces can be transformed to the common basis connected with the sliding path, i.e., to $\{\mathbf{v}, \mathbf{n}\}$, see Fig. 8. After transformation, the tensor $\overset{(s)}{\mathbf{C}}_1$ is given by

$$\begin{aligned}\overset{(s)}{\mathbf{C}}_1 = {} & [\overset{(s)}{C}{}^{11}(\overset{(s)}{B}_{11})^2 + \overset{(s)}{C}{}^{22}(\overset{(s)}{B}_{21})^2]\mathbf{v} \otimes \mathbf{v} + (\overset{(s)}{C}{}^{11}\ \overset{(s)}{B}_{11}\ \overset{(s)}{B}_{12} + \overset{(s)}{C}{}^{22}\ \overset{(s)}{B}_{21}\ \overset{(s)}{B}_{22})(\mathbf{v} \otimes \mathbf{n} + \mathbf{n} \otimes \mathbf{v}) \\ & + [\overset{(s)}{C}{}^{11}(\overset{(s)}{B}_{12})^2 + \overset{(s)}{C}{}^{22}(\overset{(s)}{B}_{22})^2]\mathbf{n} \otimes \mathbf{n}.\end{aligned} \tag{69}$$

The transformation coefficients B_{ij} $(i,j = 1,2)$ are defined by (14).

Taking into account (63)–(69), the resultant friction force at the contact of two surfaces can be expressed by

$$\mathbf{t}_{AB} = -N\left[\overset{(AB)}{\mathbf{C}}_1\,\mathbf{v} + \overset{(AB)}{\mathbf{E}}_1\,\frac{\mathbf{n}}{\rho}\right], \tag{70}$$

where

$$\overset{(AB)}{\mathbf{C}}_1 = \kappa\left[\overset{(A)}{\mathbf{C}}_1 + \overset{(B)}{\mathbf{C}}_1\right]. \tag{71}$$

The tensors $\overset{(A)}{\mathbf{E}}_1$ and $\overset{(B)}{\mathbf{E}}_1$ have the tensor bases composed of the sliding path unit vectors $\mathbf{v}$ and $\mathbf{n}$. Therefore, their components can be added without any transformation, i.e.,

$$\overset{(AB)}{\mathbf{E}}_1 = \kappa[\overset{(A)}{\mathbf{E}}_1 + \overset{(B)}{\mathbf{E}}_1] = \kappa[(\overset{(A)}{E}{}^{12} + \overset{(B)}{E}{}^{12})\mathbf{v}\otimes\mathbf{n} + (\overset{(A)}{E}{}^{22} + \overset{(B)}{E}{}^{22})\mathbf{n}\otimes\mathbf{n}]. \tag{72}$$

We consider three examples of the composed two surfaces.

First example. The composition of two surfaces (A) and (B) with two inhomogeneous friction properties in the form of concentric circles conserves the axial symmetry, if the centers of the concentric circles coincide. The axial symmetry implies that the coefficients of the transformation of the unit vectors $\{\overset{(s)}{\mathbf{k}}_1, \overset{(s)}{\mathbf{k}}_2\}$ to the basis $\{\mathbf{v},\mathbf{n}\}$ are identical for both the surfaces

$$\overset{(A)}{B}_{ij} = \overset{(B)}{B}_{ij} \equiv B_{ij}, \quad i,j = 1,2. \tag{73}$$

Hence, the resultant friction tensor (71) takes the following form:

$$\begin{aligned}\overset{(AB)}{\mathbf{C}}_1 = \kappa\{&[\overset{(AB)}{C}{}^{11}(B_{11})^2 + \overset{(AB)}{C}{}^{22}(B_{21})^2]\mathbf{v}\otimes\mathbf{v} + (\overset{(AB)}{C}{}^{11}B_{11}B_{12} + \overset{(AB)}{C}{}^{22}B_{21}B_{22})(\mathbf{v}\otimes\mathbf{n} + \mathbf{n}\otimes\mathbf{v})\\ &+ [\overset{(AB)}{C}{}^{11}(B_{12})^2 + \overset{(AB)}{C}{}^{22}(B_{22})^2]\mathbf{n}\otimes\mathbf{n}\},\end{aligned} \tag{74}$$

where

$$\overset{(AB)}{C}{}^{11} = \overset{(A)}{C}{}^{11} + \overset{(B)}{C}{}^{11}, \tag{75}$$

$$\overset{(AB)}{C}{}^{22} = \overset{(A)}{C}{}^{22} + \overset{(B)}{C}{}^{22}. \tag{76}$$

Second example. If the surfaces (A) and (B) are composed on the manner that the centers of the concentric circles do not coincide, then the unit vectors $\{\overset{(s)}{\mathbf{k}}_1, \overset{(s)}{\mathbf{k}}_2\}$ relating to the physical properties of the surfaces have different orientations with respect to the basis $\{\mathbf{v},\mathbf{n}\}$, for different surfaces. Hence, the transformation coefficients for the surfaces (A) and (B) have different values

$$\overset{(A)}{B}_{ij} \neq \overset{(B)}{B}_{ij}. \tag{77}$$

In this case, the resultant friction tensor $\overset{(AB)}{\mathbf{C}}_1$ is defined by (71) and (69). In general, the resultant friction of the composed surfaces is non-homogeneous.

Third example. Let us consider the composition of the surface (A) with non-homogeneous friction properties in the form of concentric circles (see Fig. 12) and the surface (B) with homogeneous anisotropic friction defined by the following tensor:

$$\overset{(B)}{\mathbf{C}}_1 = \overset{(B)}{C}{}^{ij}\,\overset{(B)}{\mathbf{k}}_i\otimes\overset{(B)}{\mathbf{k}}_j, \quad i,j,= 1,2. \tag{78}$$

With the aid of the second order tensor (78) we can define: orthotropic, anisotropic and isotropic homogeneous friction depending on the representation of the tensor $\mathbf{C}_1$ (see Table 1). In the case of the homogeneous friction $\overset{(B)}{\mathbf{E}}_1 = \mathbf{0}$. The unit vectors $\{\overset{(B)}{\mathbf{k}}_1, \overset{(B)}{\mathbf{k}}_2\}$ can be transformed according to the rule (13). Then, the transformation coefficients $\overset{(s)}{B}_{ij}$ have different values for the surfaces (A) and (B).

Property 2. *The symmetry group of the resultant friction* $\mathbf{t}_{AB}$ *in the contact of two surfaces is equal to an intersection (product) of the symmetry groups for the surfaces* (A) *and* (B)

$$\mathcal{G}(\mathbf{t}_{AB}) = \mathcal{G}(\overset{(A)}{\mathbf{t}}) \cap \mathcal{G}(\overset{(B)}{\mathbf{t}}). \tag{79}$$

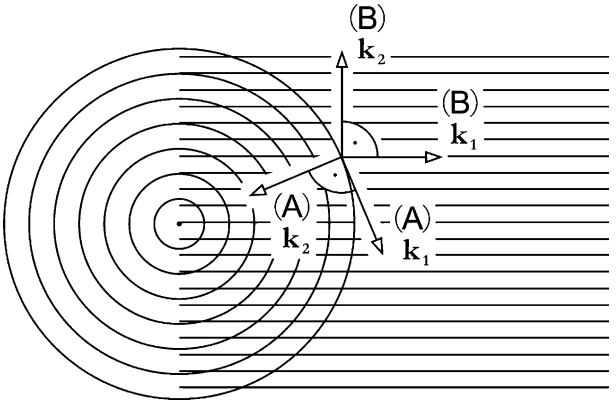

Fig. 12. The composition of two surfaces: surface (A) with inhomogeneous anisotropic properties in the form of concentric circles, surface (B) with homogeneous orthotropic properties.

The resultant symmetry, in general, has a number of elements equal to the order of the symmetry group with the lower number of symmetry generators. It acts in any case of the composed two friction inhomogeneities. The resultant friction $\mathbf{t}_{AB}$ calculated with the aid of the relation (57) has the symmetry properties which are described by the rule (79).

The non-homogeneous friction composed with the homogeneous gives the non-homogeneous friction as the composition result. Then, the intersection of the symmetry groups with respect to translations δ is given by

$$\{\mathbf{T}^{\delta}, \delta = 0\} \cap \{\mathbf{T}^{\delta}, \delta \in \langle 0, \infty)\} = \{\mathbf{T}^{\delta}, \delta = 0\}, \tag{80}$$

where $\delta = 0$ means no translations, $\delta \in \langle 0, \infty)$ denotes any translation along any axis. The contact of the surface with non-homogeneous anisotropic friction in the form of concentric circles and the surface with homogeneous anisotropic friction has non-homogeneous anisotropic behaviour.

If the homogeneous friction symmetry properties of the surface (B) are defined by the orthotropic friction group or by the anisotropic friction group, then the intersection with the axial symmetry group of the surface (A) is equal to the anisotropic symmetry group, i.e.,

$$\{\mathbf{R}_c^{\phi}\} \cap \{\pm\mathbf{1}, \mathbf{J}_{m_1}, \mathbf{J}_{m_2}\} = \{\pm\mathbf{1}\}, \tag{81}$$

$$\{\mathbf{R}_c^{\phi}\} \cap \{\pm\mathbf{1}\} = \{\pm\mathbf{1}\}. \tag{82}$$

The intersection of the axial symmetry with the isotropy defined by the full orthogonal group $\mathcal{O}$ gives the axial symmetry

$$\{\mathbf{R}_c^{\phi}\} \cap \mathcal{O} = \{\mathbf{R}_c^{\phi}\}. \tag{83}$$

The contact of two surfaces with the non-homogeneous axi-symmetric friction properties is described by the axial symmetry group (if the centers of the concentric circles coincide)

$$\{\mathbf{R}_c^{\phi}\} \cap \{\mathbf{R}_c^{\phi}\} = \{\mathbf{R}_c^{\phi}\}. \tag{84}$$

If the surfaces (A) and (B) are composed in the manner that the centers of the concentric circles do not coincide, then the contact has the symmetry group composed of the identity and a mirror reflection with respect to a plane crossing the centers of the circles and normal to the contact surface.

7. Second-order descriptions of anisotropic and heterogeneous friction

In the second-order polynomial formulation, the friction force function of the form (6) can be represented as follows:

$$\mathbf{t} = -N\left\{\mathbf{C}_1\mathbf{v} + \mathbf{C}_2\cdot(\mathbf{v}\otimes\mathbf{v}\otimes\mathbf{v}) + \mathbf{E}_1\mathbf{n}\frac{1}{\rho} + \mathbf{E}_2\cdot\left[(\mathbf{v}\otimes\mathbf{v}\otimes\mathbf{n})\frac{1}{\rho} + (\mathbf{n}\otimes\mathbf{v}\otimes\mathbf{v})\frac{1}{\rho} + (\mathbf{v}\otimes\mathbf{n}\otimes\mathbf{v})\frac{1}{\rho} + (\mathbf{v}\otimes\mathbf{n}\otimes\mathbf{n})\frac{1}{\rho^2} + (\mathbf{n}\otimes\mathbf{n}\otimes\mathbf{v})\frac{1}{\rho^2} + (\mathbf{n}\otimes\mathbf{v}\otimes\mathbf{n})\frac{1}{\rho^2} + (\mathbf{n}\otimes\mathbf{n}\otimes\mathbf{n})\frac{1}{\rho^3}\right]\right\}, \tag{85}$$

with the following fourth-order friction tensors:

$$\mathbf{C}_2(\mathbf{X}) = C^{ijkl}\mathbf{k}_i\otimes\mathbf{k}_j\otimes\mathbf{k}_k\otimes\mathbf{k}_l, \quad i,j,k,l=1,2, \quad C^{ijkl}=\text{const}, \quad \mathbf{k}_i=\mathbf{k}_i(\mathbf{X}),$$
$$\mathbf{C}_2\in\mathscr{T}_4=\mathscr{E}_2\otimes\mathscr{E}_2\otimes\mathscr{E}_2\otimes\mathscr{E}_2, \tag{86}$$

$$\mathbf{E}_2 = E^{ijkl}\mathbf{e}_i\otimes\mathbf{e}_j\otimes\mathbf{e}_k\otimes\mathbf{e}_l, \quad E^{ijkl}\neq\text{const}, \quad \{\mathbf{e}_1,\mathbf{e}_2\}\equiv\{\mathbf{v},\mathbf{n}\}, \quad \mathbf{E}_2\in\mathscr{T}_4. \tag{87}$$

In Eq. (85), the tensor $\mathbf{E}_2$ is contracted with third-order tensors composed by all combinations of $\mathbf{v}$ and $\mathbf{n}/\rho$ (with an exception of $\mathbf{v}\otimes\mathbf{v}\otimes\mathbf{v}$). Vectors $(\mathbf{v},\mathbf{n}/\rho)$ and the third-order tensors composed by these vectors are independent variables of the friction equation (85). The second-order tensors $(\mathbf{C}_1,\mathbf{E}_1)$ and the fourth-order tensors $(\mathbf{C}_2,\mathbf{E}_2)$ are equation coefficients. The tensor $\mathbf{E}_2$ describes the additional friction and the motion constraints which depend on first, second and third powers of the sliding path curvature. $\mathbf{C}_2$ defines other types of frictional anisotropy and inhomogeneity (e.g., tetragonal anisotropy). The tensor $\mathbf{C}_2$ can be transformed to the tensor basis composed by the unit vectors $\{\mathbf{v},\mathbf{n}\}$ taking into account the transformation rule (13).

Anisotropic, tetragonal anisotropic, orthotropic, isotropic and axi-symmetric friction can be distinguished with the aid of the friction tensor $\mathbf{C}_2$ and the symmetry groups, see Table 3 and Zmitrowicz

Table 3
Nonlinear models of anisotropic friction

Type of friction anisotropy	Symmetry elements	Restrictions on the friction tensor $\mathbf{C}_2$	Coefficients of the tensor $\mathbf{C}_2$	Restrictions on the coefficients
Isotropic	$\mathscr{O}$	$\mathbf{C}_2 = C^{1111}\mathbf{k}_i\mathbf{k}_j\mathbf{k}_i\mathbf{k}_j$, $i,j=1,2$	$C^{1111}=C^{2222}$ $=C^{2121}=C^{1212}$	$C^{1111}\geqslant 0$
Orthotropic	$\pm\mathbf{1}$, $\mathbf{J}_{m1}$, $\mathbf{J}_{m2}$	$\mathbf{C}_2 = C^{1111}\mathbf{k}_1\mathbf{k}_i\mathbf{k}_1\mathbf{k}_i$ $+C^{2222}\mathbf{k}_2\mathbf{k}_i\mathbf{k}_2\mathbf{k}_i$, $i=1,2$	$C^{1111}=C^{1212}$, $C^{2222}=C^{2121}$	$C^{1111}\cos^2\alpha_v + C^{2222}\sin^2\alpha_v\geqslant 0$, $\alpha_v\in<0,2\pi>$
Anisotropic	$\pm\mathbf{1}$	None	C^{1111}, C^{1122}, C^{1121}, C^{1112}, C^{2211}, C^{2222}, C^{2221}, C^{2212}, C^{2111}, C^{2122}, C^{2121}, C^{2112}, C^{1211}, C^{1222}, C^{1221}, C^{1212}	$C^{ijkl}v_iv_jv_kv_l\geqslant 0$, $i,j,k,l=1,2$, $v_1=\cos\alpha_v$, $v_2=\sin\alpha_v$
Tetragonal anisotropic	$+\mathbf{1},\mathbf{R}_n^{\pi/2}$, $\mathbf{J}_{m1}$, $\mathbf{J}_{m2}$, $\mathbf{J}_{m3}$, $\mathbf{J}_{m4}$	$\mathbf{C}_2 = C^{1111}\mathbf{k}_i\mathbf{k}_i\mathbf{k}_i\mathbf{k}_i$ $+C^{2112}\mathbf{k}_i\mathbf{k}_j\mathbf{k}_j\mathbf{k}_i$ $+C^{1122}\mathbf{k}_i\mathbf{k}_i\mathbf{k}_j\mathbf{k}_j$ $+C^{2121}\mathbf{k}_i\mathbf{k}_j\mathbf{k}_i\mathbf{k}_j$, $i\neq j$, $i,j=1,2$	$C^{1111}=C^{2222}$, C^{1122} $=C^{2211}$, $C^{2121}=C^{1212}$, $C^{2112}=C^{1221}$	$C^{1111}(\cos^4\alpha_v+\sin^4\alpha_v)+$ $2(C^{1122}+C^{2121}+C^{2112})\times$ $\cos^2\alpha_v\sin^2\alpha_v\geqslant 0$, $\alpha_v\in\langle 0,2\pi\rangle$
Axisymmetric	$\mathbf{R}_n^{\phi}$ $\phi\in\langle 0,2\pi\rangle$	$\mathbf{C}_2 =$ *isotropic tensor plus* $(-1)^{i+1}C^{1121}\mathbf{k}_i\mathbf{k}_i\mathbf{k}_j\mathbf{k}_i$ $+(-1)^{i+1}C^{1121}\mathbf{k}_i\mathbf{k}_j\mathbf{k}_j\mathbf{k}_j$, $i\neq j$, $i,j=1,2$	$C^{1111}=C^{2222}=C^{2121}$ $=C^{1212}$, $C^{1121}=-C^{2111}$ $=-C^{2212}=C^{1222}$	$C^{1111}\geqslant 0$, $C^{1121}\in\mathscr{R}$

(1989). The symmetry group $\mathcal{G}(\mathbf{C}_2)$ of the friction tensor $\mathbf{C}_2$ is the subgroup of the full orthogonal group $\mathcal{O}$ and it satisfies the following relation:

$$\mathcal{G}(\mathbf{C}_2) = \left\{ \mathbf{R} : \mathbf{R} \in \mathcal{O}, \left(\overset{4}{\underset{1}{\otimes}} \mathbf{R} \right) \cdot \mathbf{C}_2 = \mathbf{C}_2 \right\}, \tag{88}$$

where $\overset{4}{\underset{1}{\otimes}}$ denotes the following contraction:

$$\left(\overset{4}{\underset{1}{\otimes}} \mathbf{R} \right) \cdot \mathbf{C}_2 = C^{ijkl} \mathbf{R}\mathbf{k}_i \otimes \mathbf{R}\mathbf{k}_j \otimes \mathbf{R}\mathbf{k}_k \otimes \mathbf{R}\mathbf{k}_l. \tag{89}$$

Comparing tensor components before and after the symmetry transformation, one can obtain a set of equations connecting some of them. It enables to establish the set of independent components for $\mathbf{C}_2$ in various cases. Representations of the tensor $\mathbf{C}_2$ are as follows.

(a) *Tetragonal anisotropy*. It has four independent coefficients C^{1111}, C^{1122}, C^{2121} and C^{2112} arranged in the following table:

$$[\mathbf{C}_2] = \begin{array}{c} \\ 11 \\ 22 \\ 21 \\ 12 \end{array} \begin{array}{c} \begin{array}{cccc} 11 & 22 & 21 & 12 \end{array} \\ \begin{pmatrix} C^{1111} & C^{1122} & 0 & 0 \\ C^{1122} & C^{1111} & 0 & 0 \\ 0 & 0 & C^{2121} & C^{2112} \\ 0 & 0 & C^{2112} & C^{2121} \end{pmatrix} \end{array}. \tag{90}$$

The tetragonal anisotropic friction tensor is described by

$$\begin{aligned} \mathbf{C}_2 = {} & C^{1111} \mathbf{k}_i \otimes \mathbf{k}_i \otimes \mathbf{k}_i \otimes \mathbf{k}_i + C^{2112} \mathbf{k}_i \otimes \mathbf{k}_j \otimes \mathbf{k}_j \otimes \mathbf{k}_i + C^{1122} \mathbf{k}_i \otimes \mathbf{k}_i \otimes \mathbf{k}_j \otimes \mathbf{k}_j \\ & + C^{2121} \mathbf{k}_i \otimes \mathbf{k}_j \otimes \mathbf{k}_i \otimes \mathbf{k}_j, \quad i \neq j, \ \ i,j = 1,2. \end{aligned} \tag{91}$$

Its group of symmetry has the following elements: identity, rotations with the angle $\pi/2$ and four mirror reflections with respect to four principal directions, i.e.,

$$\mathcal{G}(\mathbf{C}_2) = \{ +\mathbf{1}, \mathbf{R}_n^{\pi/2}, \mathbf{J}_{m_1}, \mathbf{J}_{m_2}, \mathbf{J}_{m_3}, \mathbf{J}_{m_4} \}. \tag{92}$$

(b) *Orthotropy*. The tensor is described by two independent coefficients C^{1111} and C^{2222} in the following table:

$$[\mathbf{C}_2] = \begin{array}{c} \\ 11 \\ 22 \\ 21 \\ 12 \end{array} \begin{array}{c} \begin{array}{cccc} 11 & 22 & 21 & 12 \end{array} \\ \begin{pmatrix} C^{1111} & 0 & 0 & 0 \\ 0 & C^{2222} & 0 & 0 \\ 0 & 0 & C^{2222} & 0 \\ 0 & 0 & 0 & C^{1111} \end{pmatrix} \end{array}. \tag{93}$$

(c) *Isotropy*. The tensor is described by one independent coefficient C^{1111} as follows:

$$[\mathbf{C}_2] = \begin{array}{c} \\ 11 \\ 22 \\ 21 \\ 12 \end{array} \begin{array}{c} \begin{array}{cccc} 11 & 22 & 21 & 12 \end{array} \\ \begin{pmatrix} C^{1111} & 0 & 0 & 0 \\ 0 & C^{1111} & 0 & 0 \\ 0 & 0 & C^{1111} & 0 \\ 0 & 0 & 0 & C^{1111} \end{pmatrix} \end{array}. \tag{94}$$

(d) *Axial-symmetry*. The tensor has two independent coefficients C^{1111} and C^{1121} arranged in the table

$$[\mathbf{C}_2] = \begin{array}{c} \\ 11 \\ 22 \\ 21 \\ 12 \end{array} \begin{array}{c} \begin{array}{cccc} 11 & 22 & 21 & 12 \end{array} \\ \begin{pmatrix} C^{1111} & 0 & C^{1121} & 0 \\ 0 & C^{1111} & 0 & -C^{1121} \\ -C^{1121} & 0 & C^{1111} & 0 \\ 0 & C^{1121} & 0 & C^{1111} \end{pmatrix} \end{array}. \tag{95}$$

In the general case, the representation of the fourth-order tensor $\mathbf{E}_2$ is given by 16 coefficients, i.e.,

$$[\mathbf{E}_2] = \begin{array}{c} \\ 11 \\ 22 \\ 21 \\ 12 \end{array} \begin{array}{c} \begin{array}{cccc} 11 & 22 & 21 & 12 \end{array} \\ \begin{pmatrix} E^{1111} & E^{1122} & E^{1121} & E^{1112} \\ E^{2211} & E^{2222} & E^{2221} & E^{2212} \\ E^{2111} & E^{2122} & E^{2121} & E^{2112} \\ E^{1211} & E^{1222} & E^{1221} & E^{1212} \end{pmatrix} \end{array}. \tag{96}$$

The unit vectors $\mathbf{v}$ and $\mathbf{n}$ compose its tensor basis. Hence, the contraction of the tensor $\mathbf{E}_2$ and the independent variables (85) gives the following result:

$$\begin{aligned} &\mathbf{E}_2 \cdot \left[(\mathbf{v}\otimes\mathbf{v}\otimes\mathbf{n})\frac{1}{\rho} + \cdots + (\mathbf{n}\otimes\mathbf{n}\otimes\mathbf{n})\frac{1}{\rho^3} \right] \\ &\quad = \left[(E^{1112}+E^{1211}+E^{1121})\frac{1}{\rho} + (E^{1122}+E^{1221}+E^{1212})\frac{1}{\rho^2} + E^{1222}\frac{1}{\rho^3} \right]\mathbf{v} \\ &\qquad + \left[(E^{2112}+E^{2211}+E^{2121})\frac{1}{\rho} + (E^{2122}+E^{2221}+E^{2212})\frac{1}{\rho^2} + E^{2222}\frac{1}{\rho^3} \right]\mathbf{n}. \end{aligned} \tag{97}$$

The first component in (97) defines the additional friction (dissipative force), the second component determines the reaction to the constraints normal to the sliding path (gyroscopic force). It is seen that the contraction of the tensor $\mathbf{E}_2$ and the independent variables gives terms, which depend on the sliding path radius ρ in the first, second, or third power. Notice, that various components of the tensor $\mathbf{E}_2$ are quoted in units of m in the first, second and third power.

Taking into account the term $(\mathbf{v}\otimes\mathbf{v}\otimes\mathbf{v})$ between the independent variables of the constitutive equation (85), we get the following result of the contraction with the tensor $\mathbf{E}_2$:

$$\mathbf{E}_2 \cdot (\mathbf{v}\otimes\mathbf{v}\otimes\mathbf{v}) = E^{1111}\mathbf{v} + E^{2111}\mathbf{n}. \tag{98}$$

Both terms on the right hand side are independent on the curvature radius. Changing the path from a curve to a straight line, these terms do not disappear, since they do not depend on the curvature. Therefore they do not describe the additional friction nor the reaction to the sliding constraints. This is the reason that the component (98) is neglected in Eq. (85).

The friction force vector (85) can be decomposed into the following two components:

$$\mathbf{t} = \mathbf{t}_0 + \mathbf{t}_\rho, \tag{99}$$

where

$$\mathbf{t}_0 = -N\{\mathbf{C}_1\mathbf{v} + \mathbf{C}_2 \cdot (\mathbf{v}\otimes\mathbf{v}\otimes\mathbf{v})\}, \tag{100}$$

$$\mathbf{t}_\rho = -N\left\{ \mathbf{E}_1\mathbf{n}\frac{1}{\rho} + \mathbf{E}_2 \cdot \left[(\mathbf{v}\otimes\mathbf{v}\otimes\mathbf{n})\frac{1}{\rho} + \cdots + (\mathbf{n}\otimes\mathbf{n}\otimes\mathbf{n})\frac{1}{\rho^3} \right] \right\}. \tag{101}$$

The component $\mathbf{t}_0$ does not depend on the sliding path curvature, the component $\mathbf{t}_\rho$ depends on the trajectory curvature, and it has the following values for different curvature radii:

$$\mathbf{t}_\rho \begin{cases} = \mathbf{0} & \text{for } \rho = \infty, \\ \neq \mathbf{0} & \text{for } 0 < \rho < \infty, \\ = \infty & \text{for } \rho = 0. \end{cases} \tag{102}$$

The singular case $\rho = 0$ is physically meaningless. In many singular cases, the sliding trajectory reduces to the single point ($\rho = 0$), then there are no sliding and no dynamic friction. Furthermore, from the theoretical point of view, in corners of a zigzag path the radius of curvature ρ is equal to zero. In that case, the sliding along the zigzag line one can consider as the sliding along separate segments of straight lines with the radius of curvature equal to infinity.

The symmetry group of the friction force component $\mathbf{t}_0$ is an intersection of the symmetry groups of the friction tensors $\mathbf{C}_1$ and $\mathbf{C}_2$, i.e.,

$$\mathscr{G}(\mathbf{t}_0) = \mathscr{G}(\mathbf{C}_1, \mathbf{C}_2) = \mathscr{G}(\mathbf{C}_1) \cap \mathscr{G}(\mathbf{C}_2). \tag{103}$$

For example, the orthotropic friction force component $\mathbf{t}_0$ can be defined by isotropic tensor $\mathbf{C}_1$ and orthotropic tensor $\mathbf{C}_2$, since

$$\{\mathscr{O}\} \cap \{\pm\mathbf{1}, \mathbf{J}_{m_1}, \mathbf{J}_{m_2}\} = \{\pm\mathbf{1}, \mathbf{J}_{m_1}, \mathbf{J}_{m_2}\}. \tag{104}$$

Property 1. *The second-order friction equation (85) satisfies the axiom of objectivity.*

According to the *axiom of objectivity*, the friction constitutive relationships should be invariant with respect to any automorphisms of the Euclidean vector space $\mathscr{E}_2$ (i.e., with respect to any motion of the reference system). Automorphisms of the Euclidean space can be represented by the orthogonal tensors. Walter Noll stated, "in any system of reference, Galilean or not, the constitutive equations must be the same". Two arbitrary observers of the sliding process must recognize the same friction force vector at the contact.

The requirement of form-invariance of the friction force vector (6) is satisfied if

$$\mathbf{t}\left(N, \mathbf{R}\mathbf{v}, \mathbf{R}\frac{\mathbf{n}}{\rho}\right) = \mathbf{R}\mathbf{t}\left(N, \mathbf{v}, \frac{\mathbf{n}}{\rho}\right), \quad \forall \mathbf{R} \in \mathscr{O}, \quad \mathbf{R}^{-1} = \mathbf{R}^{\mathrm{T}}, \quad \det \mathbf{R} = \pm 1, \tag{105}$$

where the orthogonal tensor $\mathbf{R}$ describes changes of an observer. In the case of the second-order friction equation (85), the axiom of objectivity expresses as follows:

$$\begin{aligned} \mathbf{t}\left(N, \mathbf{R}\mathbf{v}, \mathbf{R}\frac{\mathbf{n}}{\rho}\right) &= -N\mathbf{R}\Big\{\mathbf{C}_1\mathbf{v} + [(\mathbf{C}_2\mathbf{v}\mathbf{R}^{\mathrm{T}})\mathbf{R}\mathbf{v}]\mathbf{v} + \mathbf{E}_1\mathbf{n}\frac{1}{\rho} + [(\mathbf{E}_2\mathbf{v}\mathbf{R}^{\mathrm{T}})\mathbf{R}\mathbf{v}]\mathbf{n}\frac{1}{\rho} + [(\mathbf{E}_2\mathbf{n}\mathbf{R}^{\mathrm{T}})\mathbf{R}\mathbf{v}]\mathbf{v}\frac{1}{\rho} \\ &\quad + [(\mathbf{E}_2\mathbf{v}\mathbf{R}^{\mathrm{T}})\mathbf{R}\mathbf{n}]\mathbf{v}\frac{1}{\rho} + [(\mathbf{E}_2\mathbf{v}\mathbf{R}^{\mathrm{T}})\mathbf{R}\mathbf{n}]\mathbf{n}\frac{1}{\rho^2} + [(\mathbf{E}_2\mathbf{n}\mathbf{R}^{\mathrm{T}})\mathbf{R}\mathbf{n}]\mathbf{v}\frac{1}{\rho^2} + [(\mathbf{E}_2\mathbf{n}\mathbf{R}^{\mathrm{T}})\mathbf{R}\mathbf{v}]\mathbf{n}\frac{1}{\rho^2} \\ &\quad + [(\mathbf{E}_2\mathbf{n}\mathbf{R}^{\mathrm{T}})\mathbf{R}\mathbf{n}]\mathbf{n}\frac{1}{\rho^3}\Big\} \\ &= \mathbf{R}\mathbf{t}\left(N, \mathbf{v}, \frac{\mathbf{n}}{\rho}\right). \end{aligned} \tag{106}$$

Here, all friction tensors $\mathbf{C}_i$, $\mathbf{E}_j$, $i,j = 1,2$ are assumed to be isotropic. The case of the isotropic tensors is more restrictive than the case of the anisotropic tensors, by virtue of the definition (105).

The principle of objectivity reduces the form of the friction constitutive equation. For example, the independent variables being even order tensors, such as

$$(\mathbf{v} \otimes \mathbf{v}), (\mathbf{v} \otimes \mathbf{n})\frac{1}{\rho}, (\mathbf{n} \otimes \mathbf{n})\frac{1}{\rho^2}, \ldots \tag{107}$$

must be neglected in the constitutive polynomial (85). They do not satisfy the condition (105).

Property 2. *The condition of power dissipated in the friction process (17) imposes restrictions on the parameters of the constitutive equation (85).*

In general, by deriving the constitutive equations, the constitutive functions are assumed to satisfy the dissipation inequality, for any regular motion. This physically motivated condition ensures satisfaction of the second law of thermodynamics in the form of inequality namely, the Clausius–Duhem inequality (*axiom of entropy production*).

The friction constitutive functions are assumed to satisfy the dissipation inequality for any sliding motion. Taking into account that $N \geqslant 0$ and $V > 0$, after substitution of the second-order friction equation (85) into the dissipation inequality (17), we obtain

$$\mathbf{v}^{\mathrm{T}}\mathbf{C}_1\mathbf{v} + \mathbf{v}^{\mathrm{T}}(\mathbf{v}^{\mathrm{T}}\mathbf{C}_2\mathbf{v})\mathbf{v} + \mathbf{v}^{\mathrm{T}}\mathbf{E}_1\mathbf{n}\frac{1}{\rho} + \mathbf{v}^{\mathrm{T}}(\mathbf{v}^{\mathrm{T}}\mathbf{E}_2\mathbf{v})\mathbf{n}\frac{1}{\rho} + \mathbf{v}^{\mathrm{T}}(\mathbf{n}^{\mathrm{T}}\mathbf{E}_2\mathbf{v})\mathbf{v}\frac{1}{\rho} + \mathbf{v}^{\mathrm{T}}(\mathbf{v}^{\mathrm{T}}\mathbf{E}_2\mathbf{n})\mathbf{v}\frac{1}{\rho} + \mathbf{v}^{\mathrm{T}}(\mathbf{v}^{\mathrm{T}}\mathbf{E}_2\mathbf{n})\mathbf{n}\frac{1}{\rho^2} + \mathbf{v}^{\mathrm{T}}(\mathbf{n}^{\mathrm{T}}\mathbf{E}_2\mathbf{n})\mathbf{v}\frac{1}{\rho^2} + \mathbf{v}^{\mathrm{T}}(\mathbf{n}^{\mathrm{T}}\mathbf{E}_2\mathbf{v})\mathbf{n}\frac{1}{\rho^2} + \mathbf{v}^{\mathrm{T}}(\mathbf{n}^{\mathrm{T}}\mathbf{E}_2\mathbf{n})\mathbf{n}\frac{1}{\rho^3} \geqslant 0, \quad \forall \mathbf{V}. \tag{108}$$

Taking the representations of the tensors $\mathbf{E}_1$ and $\mathbf{E}_2$ (19) and (96) we get

$$\mathbf{v}^{\mathrm{T}}\mathbf{C}_1\mathbf{v} + \mathbf{v}^{\mathrm{T}}(\mathbf{v}^{\mathrm{T}}\mathbf{C}_2\mathbf{v})\mathbf{v} + (E^{12} + E^{1112} + E^{1211} + E^{1121})\frac{1}{\rho} + (E^{1122} + E^{1221} + E^{1212})\frac{1}{\rho^2} + E^{1222}\frac{1}{\rho^3} \geqslant 0. \tag{109}$$

Notice that the normal component of the force $\mathbf{t}_\rho$, see Eqs. (20), (97), (101), gives the power (and the work) equal to zero.

Let us substitute

$$a = \mathbf{v}^{\mathrm{T}}\mathbf{C}_1\mathbf{v} + \mathbf{v}^{\mathrm{T}}(\mathbf{v}^{\mathrm{T}}\mathbf{C}_2\mathbf{v})\mathbf{v} + (E^{1122} + E^{1221} + E^{1212})\frac{1}{\rho^2}, \tag{110}$$

$$b = (E^{12} + E^{1112} + E^{1211} + E^{1121}) + E^{1222}\frac{1}{\rho^2}, \tag{111}$$

then the dissipation inequality (109) reduces to

$$a + \frac{1}{\rho}b \geqslant 0. \tag{112}$$

Let us consider $\rho > 0$ and the following restrictions for a and b:

$$a \geqslant 0, \quad b \geqslant 0. \tag{113}$$

Then the dissipative inequality (109) is satisfied for every sliding velocity $\mathbf{V}$ and every positive radius of curvature $\rho \in \mathscr{R}^+$.

Let us assume that $\rho > 0$ and

$$a > 0, \quad b \leqslant 0, \tag{114}$$

then the dissipative inequality is satisfied for every $\mathbf{V}$ and for some trajectories, i.e., for some values of the positive curvature radii

$$\rho \geqslant -\frac{b}{a}. \tag{115}$$

The curvature radius ρ has $\pm$ sign and the friction force depends on the positive as well negative sign of the radii. If the radius of curvature is negative $\rho < 0$ and the restrictions (113) are taken into account, then the dissipative inequality (109) is satisfied for the following radii of curvature:

$$\rho \leqslant -\frac{b}{a}. \tag{116}$$

Taking $\rho < 0$ and the restrictions (113), the dissipative inequality holds for every negative radius of curvature $\rho \in \mathscr{R}^-$.

If the sliding trajectory is a straight line ($\rho = \infty$), then the dissipation inequality is satisfied for $a \geqslant 0$ and for any b.

8. Illustrative examples of the second-order descriptions

Let us consider non-homogeneous friction properties, which form spirals in the sliding surface. This type of inhomogeneity refers to specific machining techniques of surfaces (e.g., spiral common directions of machining marks and spiral microgrooves in the surface), and to specific physical properties of materials: (a) growth spirals on crystal faces (see Tolansky, 1968), (b) microstructure evolving along spirals at the sliding surfaces of some materials (self-organization phenomenon). There are two privileged sliding trajectories in this surface, i.e., along the spirals and along curved radii perpendicular to the spirals. The sliding along spirals can occur with the lowest resistance to motion, and it can have the greatest resistance in the direction perpendicular to the spirals.

Let us assume that unit vectors $\mathbf{k}_1$ and $\mathbf{k}_2$ are tangent and normal to the spiral respectively at the given point. In the dependence on the position in the spiral, the unit vectors change their orientations with respect to the reference system. Let us consider the sliding trajectory of a material point, which coincides with the spiral. Then the following relations hold between the unit vectors:

$$\mathbf{k}_1 = \mathbf{v}, \quad \mathbf{k}_2 = \mathbf{n} \tag{117}$$

and the coefficients of the transformation matrix $\mathbf{B}$ are given by

$$B_{11} = B_{22} = 1, \quad B_{12} = B_{21} = 0. \tag{118}$$

The unit vectors $\{\mathbf{v}, \mathbf{n}\}$ describe the moving reference frame whose origin is located at the point P, see Fig. 13.

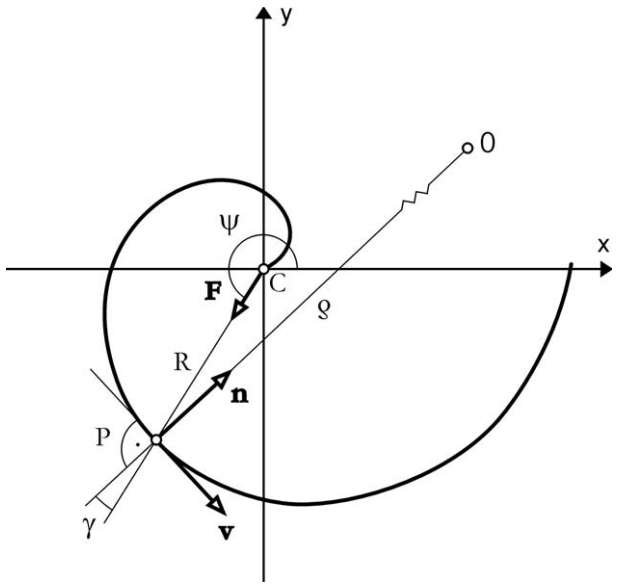

Fig. 13. The sliding trajectory of a material point in a plane with heterogeneous friction properties, which form the spiral.

The friction tensors are presented in Table 3. We have assumed the following isotropic friction tensor $\mathbf{C}_1$ and the orthotropic friction tensor $\mathbf{C}_2$

$$\mathbf{C}_1 = C^{11}(\mathbf{k}_1 \otimes \mathbf{k}_1 + \mathbf{k}_2 \otimes \mathbf{k}_2) = C^{11}\mathbf{1}, \tag{119}$$

$$\mathbf{C}_2 = C^{1111}\mathbf{k}_1 \otimes \mathbf{k}_i \otimes \mathbf{k}_1 \otimes \mathbf{k}_i + C^{2222}\mathbf{k}_2 \otimes \mathbf{k}_i \otimes \mathbf{k}_2 \otimes \mathbf{k}_i, \quad i = 1, 2, \tag{120}$$

where $\mathbf{1}$ is the identity tensor. Taking into account (100) and (117), the friction force component $\mathbf{t}_0$ is given by

$$\mathbf{t}_0 = -N(C^{11} + C^{1111})\mathbf{v}. \tag{121}$$

The tensors $\mathbf{E}_1$ and $\mathbf{E}_2$ are defined as follows:

$$\mathbf{E}_1 = E^{22}\mathbf{n} \otimes \mathbf{n}, \tag{122}$$

$$\mathbf{E}_2 = E^{2222}\mathbf{n} \otimes \mathbf{n} \otimes \mathbf{n} \otimes \mathbf{n} + E^{1212}\mathbf{v} \otimes \mathbf{n} \otimes \mathbf{v} \otimes \mathbf{n}. \tag{123}$$

Taking into account (101), the friction force component $\mathbf{t}_\rho$ is given by

$$\mathbf{t}_\rho = -N\left[\frac{E^{1212}}{\rho^2}\mathbf{v} + \left(\frac{E^{22}}{\rho} + \frac{E^{2222}}{\rho^3}\right)\mathbf{n}\right]. \tag{124}$$

Therefore, the friction force $\mathbf{t} = \mathbf{t}_0 + \mathbf{t}_\rho$ for the sliding along the spiral has the following dissipative $t^{\parallel}\mathbf{v}$ and gyroscopic $t^{\perp}\mathbf{n}$ components:

$$\mathbf{t} = -N\left[\left(C^{11} + C^{1111} + \frac{E^{1212}}{\rho^2}\right)\mathbf{v} + \left(\frac{E^{22}}{\rho} + \frac{E^{2222}}{\rho^3}\right)\mathbf{n}\right] \equiv t^{\parallel}\mathbf{v} + t^{\perp}\mathbf{n}. \tag{125}$$

The coefficients C^{11}, C^{1111}, E^{1212} and the radius of curvature ρ are restricted by the second law of thermodynamics, see Table 4. The coefficient of the dissipative friction force component depends on the second power of the curvature radius, i.e.,

$$\mu_\alpha^{\parallel}(\rho) = C^{11} + C^{1111} + \frac{E^{1212}}{\rho^2}. \tag{126}$$

In the case of kinematics dependent friction, friction is non-uniform throughout the spiral. The friction coefficient $\mu_\alpha^{\parallel}$ changes along the spiral, and it depends on the second power of the spiral curvature $(1/\rho^2)$.

Let us consider motion of a material point in a plane with non-homogeneous anisotropic friction. The motion is described by the following equation:

$$m\ddot{\mathbf{x}} = \mathbf{F} + \mathbf{t}, \tag{127}$$

where m is the mass of the material point, $\mathbf{x}$ is the position vector with the respect to the reference system Cxy. $\mathbf{F}$ is the central force of the following type:

Table 4
Heterogeneous anisotropic friction in the second-order description

Type of friction heterogeneity	Friction tensors $\mathbf{C}_1$, $\mathbf{E}_1$, $\mathbf{C}_2$, $\mathbf{E}_2$	Coefficients of the friction tensors	Restrictions on the coefficients and the radius
Spiral	$\mathbf{C}_1 = C^{11}\mathbf{1}$	C^{11}	$a + \frac{1}{\rho}b \geqslant 0$
	$\mathbf{E}_1 = E^{22}\mathbf{nn}$	E^{22}	$a = \mathbf{v}^{\mathrm{T}}\mathbf{C}_1\mathbf{v} + \mathbf{v}^{\mathrm{T}}(\mathbf{v}^{\mathrm{T}}\mathbf{C}_2\mathbf{v})\mathbf{v} + E^{1212}\frac{1}{\rho^2}$
	$\mathbf{C}_2 = C^{1111}\mathbf{k}_1\mathbf{k}_i\mathbf{k}_1\mathbf{k}_i$	$C^{1111} = C^{1212}$, $C^{2222} = C^{2121}$	$b = 0$
	$+ C^{2222}\mathbf{k}_2\mathbf{k}_i\mathbf{k}_2\mathbf{k}_i$, $i = 1, 2$		
	$\mathbf{E}_2 = E^{2222}\mathbf{nnnn} + E^{1212}\mathbf{vnvn}$	E^{2222}, E^{1212}	$E^{22} \in \mathscr{R}$, $E^{2222} \in \mathscr{R}$

$$|\mathbf{F}| = \frac{c}{R^3}, \quad c = \text{const}, \tag{128}$$

where R is the radius from the origin C to the sliding material point P (see Fig. 13). The central force is directed from the origin C to the point P. It is assumed that $\mathbf{F} \to \mathbf{0}$ if $R \to \infty$. The acceleration vector is decomposed into tangential and centrifugal accelerations as follows:

$$\ddot{\mathbf{x}} = \frac{\mathrm{d}(V\mathbf{v})}{\mathrm{d}t} = \frac{\mathrm{d}V}{\mathrm{d}t}\mathbf{v} + \frac{V^2}{\rho}\mathbf{n}, \tag{129}$$

where the time derivative of the unit vector $\mathbf{v}$ has the following form:

$$\frac{\mathrm{d}\mathbf{v}}{\mathrm{d}t} = \frac{\mathrm{d}\mathbf{v}}{\mathrm{d}s}\frac{\mathrm{d}s}{\mathrm{d}t} = V\frac{\mathrm{d}\mathbf{v}}{\mathrm{d}s}. \tag{130}$$

The motion equation given in the local basis defined by the unit vectors tangent and normal to the sliding trajectory $\{\mathbf{v},\mathbf{n}\}$ has the form as follows:

$$m\frac{\mathrm{d}V}{\mathrm{d}t} = F^{\parallel} + t^{\parallel}, \tag{131}$$

$$m\frac{V^2}{\rho} = F^{\perp} + t^{\perp}. \tag{132}$$

The tangent and normal components of the central force (see Fig. 13) are given by

$$F^{\parallel} = |\mathbf{F}|\sin\gamma\mathbf{v}, \tag{133}$$

$$F^{\perp} = -|\mathbf{F}|\cos\gamma\mathbf{n}, \tag{134}$$

where γ is the angle between the radius R and the normal direction to the trajectory.

We investigate a constrained motion of the material point, i.e., the point is constrained to move along the specified plane spiral. Here, Archimedes spiral is specified as the curved trajectory. It is given by the formula for the radius R with respect to an angle ψ (polar coordinates), i.e.,

$$R(\psi) = a\psi, \quad \psi \in \langle 0, \infty), \qquad a = \text{const}. \tag{135}$$

In this case, the radius of curvature ρ is a monotonic function of the angle ψ, and it is described as follows:

$$\rho = \frac{a(\psi^3 + 1)^{3/2}}{\psi^2 + 2}. \tag{136}$$

The angle γ is given by

$$\gamma = \frac{1}{R}\frac{\mathrm{d}R}{\mathrm{d}\psi} = \frac{1}{\psi}. \tag{137}$$

Let us introduce the sliding motion constraint normal to the spiral trajectory defined with the aid of the second motion equation (132), i.e.,

$$t^{\perp} = m\frac{V^2}{\rho} - F^{\perp}. \tag{138}$$

After substitution the gyroscopic components of the friction force (125) and the central force (128) and (134) into (138), we get

$$-N\left(\frac{E^{22}}{\rho}+\frac{E^{2222}}{\rho^3}\right)=m\frac{V^2}{\rho}-\frac{c}{R^3}\cos\gamma. \tag{139}$$

The coefficient E^{22} is assumed to be the following function of the sliding velocity:

$$E^{22}=-m\frac{V^2}{N}. \tag{140}$$

The coefficient E^{2222} is assumed to be the function of the angle ψ, i.e.,

$$E^{2222}=\frac{c\rho^3\cos\gamma}{NR^3}=\frac{c}{N}\left[\frac{(\psi^3+1)^{3/2}}{\psi(\psi^2+2)}\right]^3\cos\left(\frac{1}{\psi}\right). \tag{141}$$

According to the assumptions (140) and (141), the equation of motion in the normal direction (132) is satisfied identically, i.e., the motion in the direction normal to the spiral is constrained. In other words, the material point is constrained only to move along the spiral trajectory (an effect of a "motion by rails").

The material point moves along Archimedes spiral (135) with the sliding velocity V, i.e.,

$$V=\frac{\mathrm{d}R}{\mathrm{d}t}=a\dot{\psi} \tag{142}$$

and its time derivative described by

$$\frac{\mathrm{d}V}{\mathrm{d}t}=a\ddot{\psi}, \tag{143}$$

where ψ is the function of time. We substitute the following quantities to the motion equation (131): the tangent components of the central force (133), the friction force (126), the acceleration (143), the radius of curvature (136) and the angle (137). Then, the equation of sliding in the tangent direction to the spiral (131) is given by

$$\ddot{\psi}=\frac{1}{ma}A(\psi), \tag{144}$$

$$A(\psi)=\frac{c}{(a\psi)^3}\sin\left(\frac{1}{\psi}\right)-N\left[C^{11}+C^{1111}+E^{1212}\frac{(\psi^2+2)^2}{a^2(\psi^3+1)^3}\right]. \tag{145}$$

The material point starts sliding at the given position ψ_0 and $R_0=a\psi_0$ with the given initial velocity $V(t_0)=V_0\equiv a\dot{\psi}_0$ tangent to the spiral, i.e.,

$$\psi(t_0)=\psi_0,\quad \dot{\psi}(t_0)=\dot{\psi}_0. \tag{146}$$

By integrating the sliding velocity (142) we obtain the sliding way passed by the material point

$$s(t)=a\int_{t_0}^{t}\dot{\psi}\,\mathrm{d}\tau. \tag{147}$$

The motion equation (144) has been solved by means of the Runge–Kutta fourth-order method.

In the illustrative examples, the mass of the material point is $m=1$ kg. The normal pressure force is taken to be equal to the gravity force. The constant of the Archimedes spiral is $a=0.1$ rad^{-1} m. The coefficients of the friction tensors independent on the sliding kinematics are as follows:

$$C^{11}=0.1,\quad C^{1111}=0.05. \tag{148}$$

We considered two examples: (a) Fig. 14 shows a segment of the spiral trajectory when the friction coefficient $\mu_{\alpha}^{\|}$ increases in dependence on the curvature radius ρ (see Fig. 15), (b) Fig. 16 presents a segment of the spiral trajectory when the friction coefficient decreases with the curvature radius (see Fig. 17). The following values were taken for the constant of the central force c, the coefficient of the friction tensor dependent on the sliding kinematics E^{1212} and the motion initial conditions ψ_0, $\dot{\psi}_0$:

(a) in Figs. 14 and 15

$$c = 0.0005\ \mathrm{Nm}^3, \quad E^{1212} = -0.00025\ \mathrm{m}^2, \quad \psi_0 = 0.5\ \mathrm{rad}, \quad \dot{\psi}_0 = 5\ \mathrm{s}^{-1}\ \mathrm{rad}, \tag{149}$$

(b) in Figs. 16 and 17

$$c = 0.005\ \mathrm{Nm}^3, \quad E^{1212} = 0.0008\ \mathrm{m}^2, \quad \psi_0 = 1\ \mathrm{rad}, \quad \dot{\psi}_0 = 10\ \mathrm{s}^{-1}\ \mathrm{rad}. \tag{150}$$

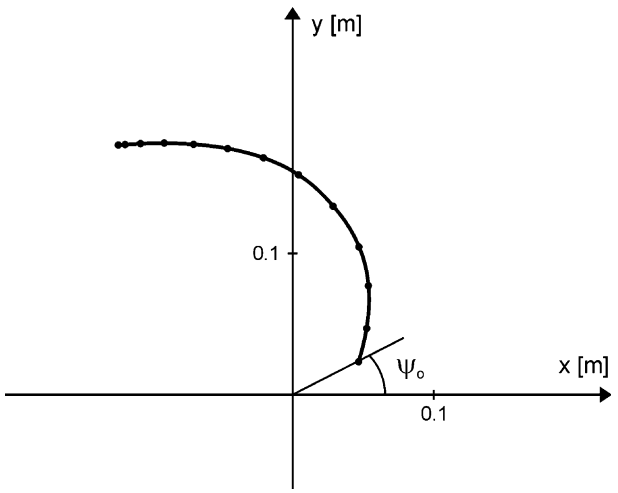

Fig. 14. The sliding trajectory of a material point along a segment of the Archimedes spiral (the small range of the curvature radii).

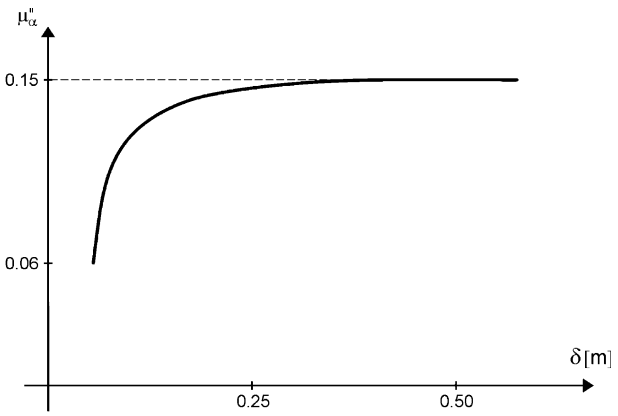

Fig. 15. Changes in the friction coefficient $\mu_{\alpha}^{\|}$ for various radii of curvature of the spiral trajectory presented in Fig. 14.

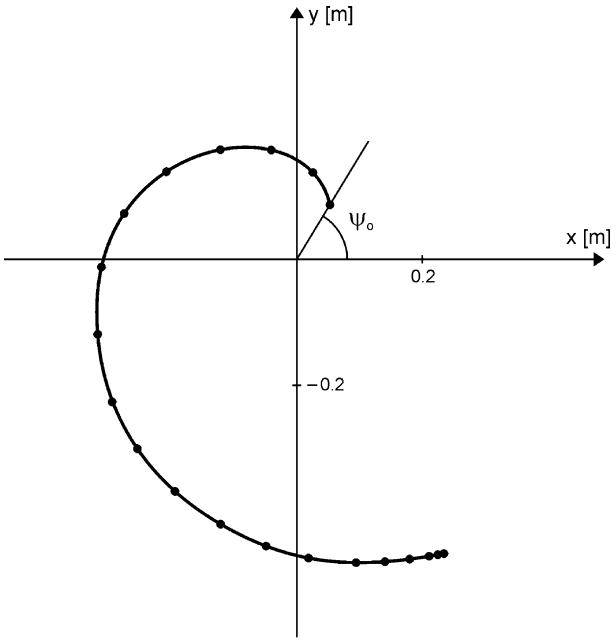

Fig. 16. The sliding trajectory of a material point along a segment of the Archimedes spiral (the large range of the curvature radii).

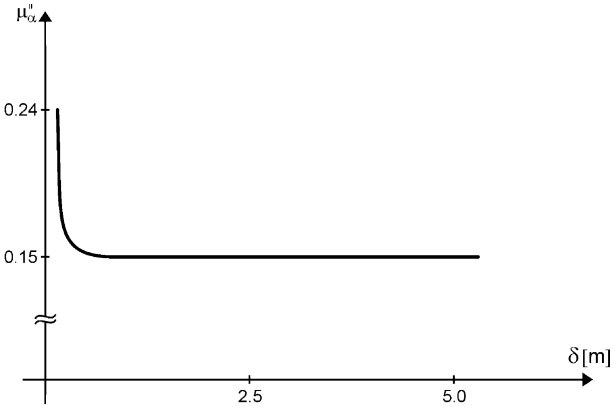

Fig. 17. Changes in the friction coefficient $\mu_z^{\parallel}$ for various radii of curvature of the spiral trajectory presented in Fig. 16.

The material point slides non-uniformly along a segment of the Archimedes spiral due to the initial velocity and the tangential components of the central and friction forces. When the radius R increases, the central force **F** decreases. Since the friction force acts, the material point dissipates the initial kinetic energy, and finally it stops. Intervals between points on the sliding trajectories plotted in Figs. 14 and 16 correspond to constant time intervals 0.04 s.

With the aid of the spiral trajectory we have a possibility to change smoothly the radii of curvature in a large range of values $\rho \in \langle 0, \infty)$. Two ranges of the curvature radii have been considered in the illustrative examples. Fig. 14 presents the trajectory for the small range of the radii ρ, i.e., from 0.053 m to 0.57 m. The trajectory shown in Fig. 16 corresponds to the large range of the radii ρ, from 0.094 m to 5.77 m. According

to Eq. (126), the friction coefficient $\mu_\alpha^{\parallel}$ depends on the second power of the sliding trajectory curvature $(1/\rho^2)$. Therefore, the friction coefficient $\mu_\alpha^{\parallel}$ is plotted as a "soft" function of ρ in the case of the small range of the curvature radii, see Fig. 15. The coefficient $\mu_\alpha^{\parallel}$ is seen as a "rapid" function of ρ in the case of the large range of the radii, see Fig. 17.

In the physical terms, it can be interpreted as follows, the friction coefficient $\mu_\alpha^{\parallel}$ modifies its value immediately after the sliding starts. There is the rapid transition of the friction coefficient from the initial value to the final value. Fig. 15 illustrates the case when the surface microstructure evolves, and the friction coefficient increases as the curvature radius also increases. Fig. 17 presents the case when the modification of the surface microstructure leads to decreasing of the friction coefficient.

The constraint force normal to the sliding path (i.e., the gyroscopic type component) can change the shape of the sliding trajectory, see detailed discussion in Zmitrowicz (1999a,b).

9. Higher-order descriptions of anisotropic and heterogeneous friction

The friction force function (6) in the most general case can be given with the aid of the following polynomial:

$$\mathbf{t} = -N\left\{\mathbf{C}_1\mathbf{v} + \mathbf{C}_2\cdot(\mathbf{v}^3) + \cdots + \mathbf{C}_n\cdot(\mathbf{v}^{2n-1}) + \mathbf{E}_1\mathbf{n}\frac{1}{\rho} + \mathbf{E}_2\cdot\left[(\mathbf{v}^2,\mathbf{n})\frac{1}{\rho} + \cdots + (\mathbf{v},\mathbf{n}^2)\frac{1}{\rho^2} + \cdots + (\mathbf{n}^3)\frac{1}{\rho^3}\right] + \cdots + \mathbf{E}_n\cdot\left[(\mathbf{v}^{2n-2},\mathbf{n})\frac{1}{\rho} + \cdots + (\mathbf{v}^{2n-3},\mathbf{n}^2)\frac{1}{\rho^2} + \cdots + (\mathbf{n}^{2n-1})\frac{1}{\rho^{2n-1}}\right]\right\} \tag{151}$$

and with the following notation of the odd order tensors as the independent variables:

$$(\mathbf{v}^p,\mathbf{n}^q)\frac{1}{\rho^q} \equiv (\underbrace{\mathbf{v}\otimes\cdots\otimes\mathbf{v}}_{p\ \text{copies}}\otimes\underbrace{\mathbf{n}\otimes\cdots\otimes\mathbf{n}}_{q\ \text{copies}})\frac{1}{\rho^q}, \quad p = 0,1,\ldots,2n-1,\ \ q = 0,1,\ldots,2n-1, \tag{152}$$

where $p+q = 3,5,\ldots,2n-1$, it is an odd number. Therefore, the higher-order terms in Eq. (151) are contractions of the following tensors:

$$\mathbf{C}_n\cdot(\mathbf{v}^{2n-1}) \equiv \mathbf{C}_n\cdot(\underbrace{\mathbf{v}\otimes\mathbf{v}\otimes\cdots\otimes\mathbf{v}}_{2n-1\ \text{copies}}), \tag{153}$$

$$\mathbf{E}_n\cdot(\mathbf{v}^{2n-2},\mathbf{n})\frac{1}{\rho} \equiv \mathbf{E}_n\cdot(\underbrace{\mathbf{v}\otimes\cdots\otimes\mathbf{v}}_{2n-2\ \text{copies}}\otimes\mathbf{n})\frac{1}{\rho}, \tag{154}$$

$$\mathbf{E}_n\cdot(\mathbf{v}^{2n-3},\mathbf{n}^2)\frac{1}{\rho^2} \equiv \mathbf{E}_n\cdot(\underbrace{\mathbf{v}\otimes\cdots\otimes\mathbf{v}}_{2n-3\ \text{copies}}\otimes\mathbf{n}\otimes\mathbf{n})\frac{1}{\rho^2}, \tag{155}$$

$$\mathbf{E}_n\cdot(\mathbf{n}^{2n-1})\frac{1}{\rho^{2n-1}} \equiv \mathbf{E}_n\cdot\underbrace{(\mathbf{n}\otimes\mathbf{n}\otimes\cdots\otimes\mathbf{n})}_{2n-1\ \text{copies}}\frac{1}{\rho^{2n-1}}. \tag{156}$$

The friction equation in polynomial form as shown in (151) contains terms which are contractions of the friction tensors $\mathbf{C}_i$, $\mathbf{E}_i$ $(i = 1,\ldots,n)$ and the tensors composed by $\mathbf{v}$ and $\mathbf{n}/\rho$. Initially, the tensors composed by $\mathbf{v}$ and $\mathbf{n}/\rho$ of all orders, i.e., first, second, third,…, $2n$, are taken into account in the polynomial. According to the objectivity axiom only odd terms composed by $\mathbf{v}$ and $\mathbf{n}/\rho$ may be included in the polynomial, i.e., first, third,…, $2n-1$. The friction tensors $\mathbf{C}_i$, $\mathbf{E}_i$ are of even order. This way, the polynomial (151) is defined uniquely.

Tensors of coefficients of the constitutive equation (151) are described as follows:

$$\mathbf{C}_n(\mathbf{X}) = C^{ij\cdots s}\underbrace{\mathbf{k}_i \otimes \mathbf{k}_j \otimes \cdots \otimes \mathbf{k}_s}_{2n \text{ copies}}, \quad i,j,\ldots,s = 1,2, \;\; C^{ij\cdots s} = \text{const}, \;\; \mathbf{k}_i = \mathbf{k}_i(\mathbf{X}),$$

$$\mathbf{C}_n \in \mathscr{T}_{2n} = \underbrace{\mathscr{E}_2 \otimes \cdots \otimes \mathscr{E}_2}_{2n \text{ copies}}, \tag{157}$$

$$\mathbf{E}_n = E^{ij\cdots s}\underbrace{\mathbf{e}_i \otimes \mathbf{e}_j \otimes \cdots \otimes \mathbf{e}_s}_{2n \text{ copies}}, \;\; E^{ij\cdots s} \neq \text{const}, \;\; \{\mathbf{e}_1, \mathbf{e}_2\} \equiv \{\mathbf{v}, \mathbf{n}\}, \;\; \mathbf{E}_n \in \mathscr{T}_{2n}. \tag{158}$$

Higher-order tensors $\mathbf{C}_1, \mathbf{C}_2, \ldots, \mathbf{C}_n$ in the constitutive polynomial define other types of frictional anisotropy and inhomogeneity. Tensors $\mathbf{E}_1, \mathbf{E}_2, \ldots, \mathbf{E}_n$ describe the additional resistance to sliding and the motion constraints which depend on an arbitrary power of the sliding path curvature ($1/\rho^k$, $k = 1, \ldots, 2n-1$).

Property. *The friction tensors $\mathbf{C}_1, \mathbf{C}_2, \ldots, \mathbf{C}_n$ describe the frictional anisotropy and symmetries of the friction force component $\mathbf{t}_0$ given in the higher-order descriptions.*

Let us decompose the friction force (151) into two components $\mathbf{t}_0$ and $\mathbf{t}_\rho$, in the similar way as it is given in (99). Due to the polynomial character of the constitutive relation (151), the symmetry group of the friction force component $\mathbf{t}_0$ is an intersection of the symmetry groups of the friction tensors $\mathbf{C}_1, \mathbf{C}_2, \ldots, \mathbf{C}_n$, i.e.,

$$\mathscr{G}(\mathbf{t}_0) = \mathscr{G}(\mathbf{C}_1, \mathbf{C}_2, \ldots, \mathbf{C}_n) = \mathscr{G}(\mathbf{C}_1) \cap \mathscr{G}(\mathbf{C}_2) \cap \cdots \cap \mathscr{G}(\mathbf{C}_n), \tag{159}$$

where

$$\mathscr{G}(\mathbf{C}_i) = \left\{\mathbf{R} : \mathbf{R} \in \mathscr{O}, \left(\overset{2i}{\underset{1}{\otimes}}\mathbf{R}\right) \cdot \mathbf{C}_i = \mathbf{C}_i\right\}, \quad i = 1, \ldots, n, \tag{160}$$

$$\left(\overset{2i}{\underset{1}{\otimes}}\mathbf{R}\right) \cdot \mathbf{C}_i \equiv C^{jl\cdots s}\underbrace{\mathbf{R}\mathbf{k}_j \otimes \mathbf{R}\mathbf{k}_l \otimes \cdots \otimes \mathbf{R}\mathbf{k}_s}_{2i \text{ copies}}. \tag{161}$$

Hence, the symmetry group $\mathscr{G}(\mathbf{t}_0)$ of the friction force component $\mathbf{t}_0$ is given by the set of all orthogonal tensors $\mathbf{R}$ for which the following identity holds:

$$\begin{aligned}\mathbf{t}_0 &= -N\left\{\left[\left(\overset{2}{\underset{1}{\otimes}}\mathbf{R}\right) \cdot \mathbf{C}_1\right]\mathbf{v} + \left[\left(\overset{4}{\underset{1}{\otimes}}\mathbf{R}\right) \cdot \mathbf{C}_2\right] \cdot (\mathbf{v}^3) + \cdots + \left[\left(\overset{2n}{\underset{1}{\otimes}}\mathbf{R}\right) \cdot \mathbf{C}_n\right] \cdot (\mathbf{v}^{2n-1})\right\} \\ &= -N\{\mathbf{C}_1\mathbf{v} + \mathbf{C}_2 \cdot (\mathbf{v}^3) + \cdots + \mathbf{C}_n \cdot (\mathbf{v}^{2n-1})\}.\end{aligned} \tag{162}$$

10. Other restrictions on the constitutive models

As in the continuum mechanics and thermodynamics, mathematical restrictions on the form of the friction constitutive relations arise from two axioms: (a) the material objectivity, (b) the entropy production inequality. Notice, that to provide a mathematically effective description sometimes additional mathematical restrictions on the friction models arise in solution procedures of boundary-value problems. In particular cases, the restrictions are related with questions of *existence and uniqueness of solutions*, which may place some limits, e.g., on values of the friction coefficients, see Nečas et al. (1980) and Cocu (1984).

In the continuum mechanics, restrictions on the form of the constitutive equations for materials arise from *representation theorems* (Smith, 1994) and *Curie principle* (Rychlewski, 1991). The representation theorems express the condition that constitutive laws are invariant with respect to the orthogonal transformations of the reference system. The friction force equations proposed in this study are polynomial

vector-valued functions, and the scalars (N, ρ) and the unit vectors $(\mathbf{v}, \mathbf{n})$ are independent variables. In this case, the representation theorems are satisfied. The Curie principle postulates that an "effect" has at least so many elements of symmetry as a "macroscopic cause" and a "physical law", which it produces. In the proposed polynomial friction equations, the friction force vector is the "effect", the independent variables of the friction equation are the "cause" and the polynomial functions are the "physical law". The Curie principle is satisfied, see detailed analysis of the symmetry properties.

11. Conclusions

(a) Nowadays a large body of engineering literature is devoted to the experimental observations of anisotropic and non-homogeneous friction and wear. The results of measurements depend on the type of material observed. The important point is the evolving microstructure in the sliding surfaces of some materials (polymers, layer-lattice materials, beryllium, magnesium) caused by the kinematics of sliding, i.e., the sliding path curvature. Attempts to explain experimental results are a source of inspiration to theoretical modelling of kinematics dependent friction and wear.

(b) The first-, second- and higher-order descriptions of non-homogeneous anisotropic friction are presented in this study. The sliding path curvature effects are included in the friction models. Various powers of the sliding path curvature are taken into account in the second- and higher-order friction equations.

(c) All friction constitutive equations satisfy the axiom of objectivity. The restrictions on the parameters of the equations follow from the axiom of entropy production. The symmetry groups are applied to obtain the mathematical classifications of friction anisotropies.

(d) The sliding path curvature generates the additional resistance to sliding (the dissipative type force). It can induce positive and negative additional friction, and it describes evolving friction. Furthermore, the sliding path curvature generates the constraint force normal to the sliding path (the gyroscopic type force).

(e) In this study, two types of anisotropic and non-homogeneous friction properties are considered in detail: (i) when the friction properties form (in geometrical terms) concentric circles in the sliding surface, (ii) when the friction properties form Archimedes spirals in the surface.

(f) The first-order models given in our previous studies (Zmitrowicz, 1999a,b) are completed with descriptions of friction asymmetry and the composition of different surfaces. The additive law of the composition defines inhomogeneity and anisotropy effects induced at the contact of two different surfaces.

(g) The constitutive equation governing wear and dependent on the sliding path curvature is created in the frame of Archard law. The parameters of the first-order models of friction and wear are estimated with the aid of Briscoe and Stolarski test data. The agreement between experimental data and the results generated by the models is very good.

The detailed analysis of anisotropic and heterogenous friction leads to the recognition and understanding of physical processes. Understanding and controlling friction and wear are of considerable practical importance in technology. For instance, turbine blades made with shroud ring segments at their tips may be grouped into assemblies. Zmitrowicz (1981, 1999c) investigated vibrations of the blade assemblies with dry friction at the contact between shroud segments. Vibration excitations caused by friction were examined in numerical tests by a finite element method. The anisotropic friction force created during vibrations of the blade assemblies was inclined to the sliding direction, and a coupling of vibrations due to frictional anisotropy was observed.

Acknowledgement

The financial support was provided by a grant from the State Committee for Scientific Research, Warsaw, No. 8T07A 03420.

References

Alart, P., 1992. A simple contact algorithm applied to large sliding and anisotropic friction. In: Curnier, A. (Ed.), Proceedings Contact Mechanics International Symposium. Lausanne, Switzerland, pp. 321–336.

Aleksandrovich, A.I., Vekshin, B.S., Potapov, I.N., 1983. A macroscopic analysis of anisotropic friction in a metal forming process. Izvestia Vyshich Uchebnych Zavedeni. Chernaia Metalurgia 8, 34–36 (in Russian).

Arikan, R., Murphy, S., 1991. Anisotropic wear of planar-random metal matrix composites with zinc alloy matrix. Wear 143 (1), 149–157.

Belmonte, M., Jurado, J.R., Treheux, D., Miranzo, P., 1996. Role of triboelectrification mechanism in the wear behaviour of Al_2O_3–SiC platelet composites. Wear 199 (1), 54–59.

Bhushan, B., 1995. Handbook of Micro/Nanotribology. CRC Press, Inc., Boca Raton, FL, pp. 101–107.

Bluhm, H., Schwarz, U.D., Meyer, K.-P., Wiesendanger, R., 1995. Anisotropy of sliding friction on the triglycine sulfate (0 1 0) surface. Applied Physics A: Materials Science & Processing 61 (5), 525–533.

Bowden, F.P., Tabor, D., 1956. Friction and Lubrication. Methuen & Co. Ltd., John Wiley & Sons Inc., London, New York.

Bowden, F.P., Tabor, D., 1958. The Friction and Lubrication of Solids, Part 1. Clarendon Press, Oxford.

Bowden, F.P., Tabor, D., 1964. The Friction and Lubrication of Solids, Part 2. Clarendon Press, Oxford.

Briscoe, B.J., Stolarski, T.A., 1979. Combined rotating and linear motion effects on the wear of polymers. Nature 281 (5728), 206–208.

Briscoe, B.J., Stolarski, T.A., 1981. The effect of the complex motion in the pin-on-disc machine on the friction and wear mechanism of organic polymers. In: Hebda, M., Kajdas, C., Hamilton, M. (Eds.), Proceedings of the 3rd International Tribology Congress Eurotrib 81. Wydawnictwo Komunikacji i Łączności, Warsaw, vol. IV, pp. 80–99.

Briscoe, B.J., Stolarski, T.A., 1985. Transfer wear of polymers during combined linear motion and load axis spin. Wear 104 (2), 121–137.

Briscoe, B.J., Stolarski, T.A., 1991. The influence of contact zone kinematics on wear process of polymers. Wear 149 (1–2), 233–240.

Brookes, C.A., Brookes, E.J., Xing, G., 1995. The effect of temperature on the deformation of diamond surfaces. In: Drory, M.D., Bogy, D.B., Donley, M.S., Field, J.E. (Eds.), Mechanical Behavior of Diamond and Other Forms of Carbon. Symposium Mater. Res. Soc., Pittsburgh, USA, pp. 59–71.

Buckley, D.H., Miyoshi, K., 1984. Friction and wear of ceramics. Wear 100, 333–353.

Carpick, R.W., Sasaki, D.Y., Burns, A.R., 1999. Large friction anisotropy of a polydiacetylene monolayer. Tribology Letters 7 (2/3), 79–85.

Chang, H.-W., 1983. Wear characteristics of composites: effect of fiber orientation. Wear 85 (1), 81–91.

Chvedov, D., Jones, R., Rosenfeld, A., 2003. Effect of lubricant quantity and surface topography on the frictional behaviour of can body stock. Tribology Transactions 46 (3), 339–347.

Ciring, M., Friedrich, K., Pipes, R.B., 1988. The effect of fiber-orientation on the abrasive wear behaviour of polymer composite materials. Wear 121 (2), 127–141.

Cocu, M., 1984. Existence of solutions of Signorini problems with friction. International Journal of Engineering Sciences 22 (5), 567–575.

Conti, P., 1875a. Sulla resistenza di attrito. Atti della Rendiconti Accademia dei Lincei, Anno CCLXXII, Seria 2, vol. II, 1874–75, Roma, coi Tipi del Salviucci 1875, pp. 16–200.

Conti, P., 1875b. Atti della Rendiconti Accademia dei Lincei, Seria 2, vols. 1, 2. Tavole, Roma 1875, Tav. I–XXV.

Coulomb, C.A., 1785. Théorie des machines simples, en ayant égard au frottement de leurs parties et á la roideur des cordages. Memoires de mathématique et de physique présentées á l'Académie Royale des Sciences par divers Savants, vol. 10, pp. 161–332 and five tables.

Curnier, A., 1996. Anisotropic friction experimental investigation. In: Klarbring, A., Andersson, L.-E. (Eds.), Abstracts Euromech Colloquium 351 "Systems with Coulomb friction". Linköping University, Sweden, pp. 34–35.

Cyfka, M., Hornbogen, E., 1986. Description of anisotropic wear rates of polymer-base composites. Journal of Materials Science Letters 5 (4), 424–426.

Dickrell, P.L., Sinnott, S.B., Hahn, D.W., Raravikar, N.R., Schadler, L.S., Ajayan, P.M., Sawyer, W.G., 2005. Frictional anisotropy of oriented carbon nanotube surfaces. Tribology Letters 18 (1), 59–62.

Dizdar, S., 2000. Wear transition of a lubricated sliding steel contact as a function of surface texture anisotropy and formation of boundary layers. Wear 237 (2), 205–210.

Dmitriev, N.N., 1993. The start of the motion of a material point on a plane with anisotropic friction. Vest. St.-Peterbg. Univ., Ser. I, Mat. Mekh. Astr., vol. 1, pp. 122–124 (in Russian).

Dmitriev, N.N., 2002. Motion of a disc and a ring on a plane with anisotropic friction. Trenie i Iznos 23 (1), 10–15 (in Russian).

Eliezer, Z., Khanna, V.D., Amateau, M.F., 1978. Wear mechanism in composites: a qualitative model. Wear 51 (1), 169–179.

Eliezer, Z., Khanna, V.D., Amateau, M.F., 1979. On the effect of fiber orientation on the wear of composite materials. Wear 53 (2), 387–389.

El-Sayed, A.A., El-Sherbiny, M.G., Abo-El-Ezz, A.S., Aggag, G.A., 1995. Friction and wear properties of polymeric composite materials for bearing applications. Wear 184 (1), 45–53.

El-Tayeb, N.S.M., Mostafa, I.M., 1996. The effect of laminate orientations on friction and wear mechanisms of glass reinforced polyester composite. Wear 195 (1–2), 186–191.

Exner, F., 1873. Untersuchungen über die Härte an Krystallflächen. Eine von der kaiserl. Akademie der Wissenschaften zu Wien gekrönte Preisschrift von .... Aus der k.k. Hof- und Staatsdruckerei, Wien, pp. 1–166 and 62 figures.

Eytelwein, J.U., 1808. Handbuch der Statik fester Körper mit vorzüglicher Rücksicht auf ihre Anwendung in Architektur. In der Realschulbuchhandlung, Berlin, Band 1, VII. Kapitel. Von der Reibung, pp. 224–239.

Flom, D.G., Komanduri, R., 2002. Some indentation and sliding experiments on single crystal and polycrystalline materials. Wear 252 (5–6), 401–429.

Franklin, S.E., 2001. Wear experiments with selected engineering polymers and polymer composites under dry reciprocating sliding conditions. Wear 250–251 (Part 2), 1591–1598.

Friedrich, K. (Ed.), 1993. Advances in Composite Tribology. Elsevier, Amsterdam.

Gatzen, H.H., Beck, M., 2003. Investigations on the friction force anisotropy of the silicon lattice. Wear 254 (11), 1122–1126.

Gellman, A.J., Ko, J.S., 2001. The current status of tribological surface science. Tribology Letters 10 (1–2), 39–44.

Gerstner von, F.J.R., 1831. Handbuch der Mechanik von . . .aufgesetzt, mit Beiträgen von neuern englischen Konstrukzionen vermehrt und herausgegeben von .... Gedruct bei Johann Spurny, Prag, Erster Band. Mechanik fester Körper, V. Kapitel. Wiederstände der Reibung, Unbiegsamkeit der Seile und ihr Einfluss auf den Effect der Maschinen, pp. 489–532.

Glitrow, J.P., Lancaster, J.K., 1967. Friction and wear of polymers reinforced with carbon fibers. Nature 214 (5093), 1106–1107.

Glodež, S., Ren, Z., Flašker, J., 1998. Simulation of surface pitting due to contact loading. International Journal of Numerical Methods in Engineering 43 (1), 33–50.

Gourdon, D., Burnham, N.A., Kulik, A., Dupas, E., Oulevey, F., Stamou, D., Liley, M., Dienes, Z., Vogel, H., Duschl, C., 1997. The dependence of friction anisotropies on the molecular organisation of LB films as observed by AFM. Tribology Letters 3 (4), 317–324.

Grillo, S.E., Field, J.E., van Bouwelen, F.M., 2000. Diamond polishing: the dependency of friction and wear on load and crystal orientation. Journal of Physics D: Applied Physics 33 (8), 985–990.

Guan, N., Thunell, B., Lyth, K., 1983. On the friction between steel and some common Swedish wood species. Holz als Roh- und Werkstoff 41, 55–60.

Hamel, G., 1949. Theoretische Mechanik. Eine einheitliche Einführung in die gesamte Mechanik. Springer, Berlin, second ed., Springer, Berlin, 1967, p. 73.

Hazel, J., Stone, M., Grace, M.S., Tsukruk, V.V., 1999. Nanoscale design of snake skin for reptation locomotions via friction anisotropy. Journal of Biomechanics 32, 477–484.

He, Q.-C., Curnier, A., 1993. Anisotropic dry friction between two orthotropic surfaces undergoing large displacements. European Journal of Mechanics, A/Solids 12 (5), 631–666.

Hirano, M., Shinjo, K., 1993. Superlubricity and frictional anisotropy. Wear 168 (1–2), 121–125.

Hirano, M., Shinjo, K., Kaneko, R., Murata, Y., 1991. Anisotropy of frictional forces in muscovite mica. Physical Review Letters 67 (19), 2642–2645.

Hisada, K., Knobler, C.M., 2002. Microscopic friction anisotropy and asymmetry related to the molecular tilt azimuth in a monolayer of glycerol ester. Colloids and Surfaces A: Physicochemical and Engineering Aspects 198–200, 21–30.

Hjiaj, M., Feng, Z.-Q., de Saxcé, G., Mróz, Z., 2004. On the modelling of complex anisotropic frictional contact laws. International Journal of Engineering Science 42 (10), 1013–1034.

Ho, K.-C., Jeng, M.-C., 1997. Tribological characteristics of short glass fiber reinforced polycarbonate composites. Wear 206 (1–2), 60–68.

Horaguchi, I., Afaghani, J.E.D., Yamaguchi, K., Nakamoto, T., 1996. Characterization and application of the sliding wear of hardened die steel against SiC whisker-plastic composite. Wear 198 (1–2), 229–235.

Hornbogen, E., 1986. Description and wear of materials with heterogeneous and anisotropic microstructure. Wear 111 (4), 391–402.

Horng, J.H., Lin, J.F., Lee, K.Y., 1994. The effect of surface irregularities on the tribological behavior of steel rollers under rolling-sliding contact. Journal of Tribology 116 (2), 209–218.

Hutton, T.J., Johnson, D., McEvaney, B., 2001. Effects of fibre orientation on the tribology of a model carbon–carbon composite. Wear 249 (8), 647–655.

Huygens, Ch., 1690. Traité de la Lumière, Van der Aa, Leyden. English edition: Treatise on light. In: Hutchins, R.M. (Editor in Chief), Great Books of the Western World. Encyclopedia Britannica, Inc., Chicago 1952, vol. 34, pp. 545–619 (Chapter Five. On the strange refractions of Iceland crystal).

Jacobs, O., Friedrich, K., Maron, G., Schulte, K., Wagner, H.D., 1990. Fretting wear performance of glass-, carbon- and armid-fiber/epoxy and peek composites. Wear 135 (2), 207–216.

Kadijk, S.E., Broese van Groenou, A., 1990. Wear anisotropy of MnZn ferrite. Part I: Recorder and sphere-on-tape experiments. Part II: Sliding sphere experiments. Part III: A wear model. Wear 139 (1), 93–113, 115–132, 133–148.

Kajiyama, T., Tanaka, K., Ge, S.-R., Takahara, A., 1996. Morphology and mechanical properties of polymer surfaces via scanning force microscopy. Progress in Surface Science 52 (1), 1–52.

Kanagawa, I., Ogata, S., Osaki, H., 2003. Effect of temperature, humidity and crystal directions on wear of rotary heads. Tribology International 36 (4–6), 433–436.

Ko, J.S., Gellman, A.J., 2000. Friction and anisotropy at Ni(100)/Ni(100) interfaces. Langmuir 16 (22), 8343–8351.

Komanduri, R., Chandrasekaran, N., Raff, L.M., 2000. MD simulation of indentation and scratching of single crystal aluminum. Wear 240 (1), 113–143.

Kragelskii, I.V., 1965. Friction and Wear. Butterworths, Washington.

Lancaster, J.K., 1966. Anisotropy in the mechanical properties of lamellar solids and its effect on wear and transfer. Wear 9, 169–188.

Lanza, G., 1901. Notes on Friction. J.S.Cushing & Co., Boston, Chapter. Morin's experiments, pp. 115–120.

Laursen, T.A., 2002. Computational Contact and Impact Mechanics: Fundamentals of Modeling Interfacial Phenomena in Nonlinear Finite Element Analysis. Springer-Verlag, Berlin, Heidelberg, pp. 211–238.

Liang, Y.N., Li, S.Z., Zhang, R.H., Li, S., 1996. Effect of fiber orientation on a graphite fiber composite in single pendulum scratching. Wear 198 (1–2), 122–128.

Liang, Y.N., Lee, S.W., Park, D.S., 1999a. Sliding behaviors of a unidirectionally oriented Si_3N_{4W}/Si_3N_4 composite. Wear 224 (1), 202–210.

Liang, Y.N., Lee, S.W., Park, D.S., 1999b. Effects of whisker distribution and sintering temperature on friction and wear of Si_3N_4-whisker-reinforced Si_3N_4-composites. Wear 225–229 (Part II), 1327–1337.

Liley, M., Gourdon, D., Stamou, D., Meseth, U., Fischer, T.M., Lautz, C., Stahlberg, H., Vogel, H., Burnham, N.A., Duschl, C., 1998. Friction anisotropy and asymmetry of a compliant monolayer induced by a small molecular tilt. Science 280 (5361), 273–275.

Lu, Z., Friedrich, K., Pannhorst, W., Heinz, J., 1993. Wear and friction of a unidirectional carbon fiber–glass matrix composite against various counterparts. Wear 162–164 (Part B), 1103–1113.

Mancinelli, C.M., Gellman, A.J., 2004. Friction anisotropy at Pd(100)/Pd(100) interfaces. Langmuir 20 (5), 1680–1687.

Martin, J.M., Pascal, H., Donnet, C., Mogne, Th.L., Loubet, J.L., Epicier, Th., 1994. Superlubricity of MoS_2: crystal orientation mechanisms. Surface & Coatings Technology 68/69, 427–432.

Mesfar, W., Shirazi-Adl, A., Dammak, M., 2003. Modeling of biomedical interfaces with nonlinear friction properties. Bio-Medical Materials and Engineering 13 (1), 91–101.

Michałowski, R., Mróz, Z., 1978. Associated and non-associated sliding rules in contact friction problems. Archives of Mechanics 30 (3), 259–276.

Minford, E., Prewo, K., 1985. Friction and wear of graphite–fiber-reinforced glass matrix composites. Wear 102 (3), 253–264.

Miyoshi, K., Buckley, D.H., 1982. Anisotropic tribological properties of SiC. Wear 75 (1), 253–268.

Moreau, J.J., 1988. Unilateral contact and dry friction in finite freedom dynamics. In: Moreau, J.J., Panagiotopoulos, P.D. (Eds.), Nonsmooth Mechanics and Applications, CISM Courses and Lectures, 302. Springer-Verlag, Wien, pp. 1–82.

Morin, A., 1832. Nouvelles expériences sur le frottement, faites a Metz en 1831, par .... Bachelier, imprimeur-libraire, Paris, pp. 1–128, Tables 1–9.

Morin, A., 1834. Nouvelles expériences sur le frottement, faites a Metz en 1832, par .... Bachelier, imprimeur-libraire, Paris, pp. 1–104, Tables 10–13.

Morin, A., 1835. Nouvelles expériences sur le frottement, faites a Metz en 1833, par .... Bachelier, imprimeur-libraire, Paris, pp. 1–143, Tables 14–17.

Morin, A., 1843. Aide-mémoire de mécanique pratique a l'usage des officiers d'artillerie et des ingénieurs civils et militaires ... Troisiéme édition .... Librairie scientifique-industrielle de L.Mathias (Augustin), Paris, Chapitre. Du frottement, pp. 305–336.

Morin, A., 1844. Morin's Hilfsbuch des praktischen Mechanikers zum gebrauche von Artillerie-offizieren, Civil- und Militäringenieuren deutsch bearbeitet von G.Holzman. Druck und Verlag Christian Teodor Groos, Karlsruhe, zweite Auflage, Kapitel. Von der Reibung, pp. 213–231.

Morin, A., 1846. Leçons de mécanique pratique a l'usage des auditeurs des cours du conservatoire des arts et métiers, et des sous-officiers et ouvriers d'artillerie, par ..., 1er Partie. Notions fondamentales et données d'expérience. Librairie scientifique-industrielle

de L. Mathias (Augustin), Paris, Chapitre. Des résistance passives dans les machines, pp. 213–243, Chapitre. De la raideur des cordes, pp. 244–261.

Morin, A., 1858. Guidebook of rules in applied mechanics to practical use for engineers, mechanicians, civil engineers and for all technicians written taking into account works and experiences of most celebrated engineers by ... Józef Sporny translated and published from the last 4th edition. In Henryk Natanson bookshop, Warsaw, Chapter. Friction and stiffness of ropes, pp. 325–357 (in Polish).

Morin, A., 1859. Practical guidebook for engineers, mechanicians, civil engineers and artillerymen by Artur Morin. Translated and completed with later experiences ... and tables of a transition from metric to foot units by Bronisław Marczewski. Published by the translator in J. Jaworski printing-house, Warsaw, Chapter. On friction, pp. 315–340 (in Polish).

Mróz, Z., 2002. Contact friction models and stability problems. In: Martins, J.A.C., Raous, M. (Eds.), Friction and Instabilities, CISM Courses and Lectures, 457. Springer, Wien, New York, pp. 179–232.

Mróz, Z., Stupkiewicz, S., 1994. An anisotropic friction and wear model. International Journal of Solids and Structures 31 (8), 1113–1131.

Nayeb-Hashemi, H., Blucher, J.T., Mirages, J., 1991. Friction and wear behavior of aluminium-graphite composites as a function of interface and fiber direction. Wear 150 (1–2), 21–39.

Nečas, J., Jarušek, J., Haslinger, J., 1980. On the solution of the variational inequality to the Signorini problem with small friction. Bollettino della Unione Matematica Italiana 17-B (5), 796–811.

Ohtani, T., Kamasaki, K., Tanaka, C., 2003. On abrasive wear property during three-body abrasion of wood. Wear 255 (Part I), 60–66.

Ohzono, T., Fujihira, M., 2000. Simulations of friction anisotropy on ordered organic monolayer. Tribology Letters 9 (1–2), 63–67.

Ovaert, T.C., 1997. Wear of unidirectional polymer matrix composites with fiber orientation in the plane contact. Tribology Transactions 40 (2), 227–234.

Overney, R.M., Takano, H., Fujihira, M., Paulus, W., Ringsdorf, H., 1994. Anisotropy in friction and molecular stick-slip motion. Physical Review Letters 72 (22), 3546–3549.

Pearce, R., Vancso, G.J., 1998. Frictional anisotropy and sectorization in poly(4-methyl-1-pentene) lamellar crystals studied by lateral force microscopy. Polymer 39 (26), 6743–6746.

Persson, B.N.J., 2000. Sliding Friction. Physical Principles and Applications, second ed. Springer, Berlin.

Prinz, F., Karnthaler, H.P., Kirchner, H.O.K., 1981. Study of the anisotropy of the friction stress in Cu–Al alloys. Acta Metallurgica 29 (6), 1029–1036.

Qi, Y., Cheng, Y.-T., Çağin, T., Goddard III, W.A., 2002. Friction anisotropy at Ni(100)/(100) interfaces: molecular dynamics studies. Physical Review B—Condensed Matter and Materials Physics 66 (8), 085420.

Rabinowicz, E., 1957. Direction of the friction force. Nature 179 (4569), 1073.

Rabinowicz, E., 1995. Friction and Wear of Materials, second ed. J. Wiley, New York.

Ravikiran, A., 2000a. Wear mechanism based on wear anisotropy. Tribology Transactions 43 (2), 287–292.

Ravikiran, A., 2000b. Effect of sliding conditions on formation of grain-pits due to wear anisotropy. Journal of Material Science Letters 19 (12), 1041–1043.

Riesz, C.H., Weber, H.S., 1964. Friction and wear of sapphire. In: Bryant, P.J., Lavik, M., Salomon, G. (Eds.), Mechanisms of Solid Friction. Elsevier, Amsterdam, pp. 67–81.

Roberts, J.C., 1985. Surface morphology studies in polymer–graphite/epoxy sliding. ASLE Transactions 28 (4), 503–510.

Rychlewski, J., 1991. Symmetry of Reasons and Effects. PWN, Warsaw (in Polish).

Sahin, Y., Murphy, S., 1998. The effect of sliding speed and microstructure on the dry wear properties of metal–matrix composites. Wear 214 (1), 98–106.

Saka, N., Szeto, N.K., Erturk, T., 1992. Friction and wear of fiber-reinforced metal–matrix composites. Wear 157 (2), 339–357.

Schön, J., 2000. Coefficient of friction of composite delamination surfaces. Wear 237 (1), 77–89.

Schouterden, K., Lairson, B.M., 1999. Anisotropy in wear processes measured by scanning probe microscopy. Thin Solid Films 340, 40–44.

Scott, V.D., Wilman, H., 1958. Surface re-orientation caused on metals by abrasion—its nature, origin and relation to friction and wear. Proceedings of the Royal Society, Series A Mathematical and Physical Sciences 247A (1250), 353–368.

Seal, M., 1957. The friction and wear of diamond. In: Edited by the Institution, Proceedings of the Conference on Lubrication and Wear held at the Institution of Mechanical Engineers. Published by the Institution of Mechanical Engineers, London, pp. 252–256, 801, 822.

Senouci, A., Frene, J., Zaidi, H., 1999. Wear mechanism in graphite–copper electrical sliding contact. Wear 225–229 (Part II), 949–953.

Sharpin, E.F., 1957. On friction heterogeneity in pressure metal forming. Trudy Kharskovskovo Politehnicheskovo Instituta 9 (1), 221–241 (in Russian).

Sheehan, P.E., Lieber, C.M., 1996. Nanotribology and nanofabrication of MoO_3 structures by atomic force microscopy. Science 272 (5265), 1158–1161.

Shim, H.H., Kwon, O.K., 1992. Effects of fiber orientation and humidity on friction and wear properties of graphite fibre composites. Wear 157 (1), 141–149.
Smith, G.F., 1994. Constitutive Equations for Anisotropic and Isotropic Materials. Elsevier, New York.
Sung, N.-H., Suh, N.P., 1979. Effect of fiber orientation on friction and wear of fiber reinforced polymeric composites. Wear 53 (1), 129–141.
Tabor, D., Williams, D.E., 1961. The effect of orientation on the friction of polytetrafluoroethylene. Wear 4 (5), 391–400.
Tarasov, V.V., 1999a. Simulation of anisotropic friction. Trenie i Iznos 20 (3), 300–305 (in Russian).
Tarasov, V.V., 1999b. Methodical aspects of anisotropic friction study. Trenie i Iznos 20 (6), 604–606 (in Russian).
Tolansky, S., 1960. Surface Microtopography. Longmans, London, pp. 257–266.
Tolansky, S., 1968. Microstructures of Surface using Interferometry. Edward Arnold (Publishers) Ltd., London, pp. 40–49.
Tong, J., Arnell, R.D., Ren, L.-Q., 1998. Dry sliding wear behaviour of bamboo. Wear 221 (1), 37–46.
Tripathy, B.S., Furey, M.J., 1993. Tribological behavior of unidirectional graphite–epoxy and carbon–PEEK composites. Wear 162–164 (Part A), 385–396.
Tsukizoe, T., Ohmae, N., 1975. Wear performance of unidirectionally oriented carbon–fibre-reinforced plastics. Tribology International 8 (4), 171–175.
Tusima, K., 1972. Anisotropy in friction of single crystals of ice. Low Temperature Science, Series A (Physical Sciences) 30, 211–213 (in Japanese).
Vaz, M.F., Fortes, M.A., 1998. Friction properties of cork. Journal of Materials Science 33 (8), 2087–2093.
von Mises, R., 1901–1908. Experimentelle Untersuchung der Reibung. In: Klein, F., Müller, C. (Eds.), Encyklopädie der mathematischen Wissenschaften: mit Einschluss ihrer Anwendungen, Band IV/1–2, Mechanik. B.G.Teubner, Leipzig, pp. 196–218.
Wada, N., Uchiyama, Y., 1993. Friction and wear of short-fibre-reinforced rubber composites under various sliding speeds and loads. Wear 162–164 (Part B), 930–938.
Wang, J., Whitley, B.W., Cusano, C., Conry, T.F., 1997. An experimental study of the effects of surface lay orientation on initial surface damage in point contacts. Tribology Transactions 35 (4), 583–594.
Watanabe, Y., Yamanaka, N., Fukui, Y., 1999. Wear behavior of Al–Al_3Ti composite manufactured by a centrifugal method. Metallurgical and Materials Transactions A 30 (12), 3253–3261.
Weick, B.L., Bhushan, B., 2001. The anisotropic friction characteristics of crystalline materials: a review. In: Bhushan, B. (Ed.), Fundamantals of Tribology and Bridging the Gap Between the Macro- and Micro/Nanoscales, Proceedings of the NATO Advanced Study Institute. Kluwer Academic Publishers, Dordrecht, pp. 279–297.
Wriggers, P., 2002. Computational Contact Mechanics. John Wiley & Sons Ltd., Chichester, pp. 66–71.
Xiao, Y., Matsubara, T., Wang, W.X., Takao, Y., 1998. Effect of carbon fiber direction of unidirectionally reinforced epoxy composites on frictional behavior. Journal of the Society of Materials Science Japan 47 (6), 618–624 (in Japanese).
Yamamoto, Y., Hashimoto, M., 2004. Friction and wear of water lubricated PEEK and PPS sliding contacts, Part 2. Composites with carbon or glass fibre. Wear 257 (1–2), 181–189.
Yang, J., Cowan, R.S., Winer, W.O., 1993. Prediction of failure transitions in sliding contacts by a thermomechanical wear model. Journal of Tribology 115 (3), 432–438.
Zhivov, V.S., 1965. A classification of locations on a plane with anisotropic friction. In: Kragelskii, I.V. et al. (Eds.), Theory of Friction and Wear. Izd. Nauka, Moscow, pp. 12–16 (in Russian).
Zmitrowicz, A., 1981. A vibration analysis of a turbine blade system damped by dry friction forces. International Journal of Mechanical Sciences 23 (12), 741–761.
Zmitrowicz, A., 1989. Mathematical descriptions of anisotropic friction. International Journal of Solids and Structures 25 (8), 837–862.
Zmitrowicz, A., 1992a. A constitutive modelling of centrosymmetric and non-centrosymmetric anisotropic friction. International Journal of Solids and Structures 29 (23), 3025–3043.
Zmitrowicz, A., 1992b. Illustrative examples of centrosymmetric and non-centrosymmetric anisotropic friction. International Journal of Solids and Structures 29 (23), 3045–3059.
Zmitrowicz, A., 1993. Constitutive equations for anisotropic wear. International Journal of Engineering Sciences 31 (3), 509–528.
Zmitrowicz, A., 1995. Constitutive models for anisotropic frictional heat. International Journal of Heat and Mass Transfer 38 (3), 563–574.
Zmitrowicz, A., 1998. Constitutive modelling of non-homogeneous and anisotropic friction of materials—sliding path curvature effects. In: Idelsohn, S., Oñate, E., Dvorkin, E. (Eds.), Computational Mechanics. New Trends and Applications, CD-ROM. CIMNE, Barcelona, Spain, pp. 1–21.
Zmitrowicz, A., 1999a. An equation of anisotropic friction with sliding path curvature effects. International Journal of Solids and Structures 36 (19), 2825–2848.
Zmitrowicz, A., 1999b. Illustrative examples of anisotropic friction with sliding path curvature effects. International Journal of Solids and Structures 36 (19), 2849–2863.
Zmitrowicz, A., 1999c. Vibrations of turbine blade assemblies with stick and slip conditions. In: Pfeiffer, F., Glocker, Ch. (Eds.), IUTAM Symposium on Unilateral Multibody Contacts. Kluwer Academic Publishers, Dordrecht, The Netherlands, pp. 319–329.
Zmitrowicz, A., 2003. Glaciers and laws of friction and sliding. Acta Mechanica 166 (1–4), 185–206.

Zmitrowicz, A., 2004. Evolutions of friction anisotropy and heterogeneity. In: Gutkowski, W., Kowalewski, T.A. (Eds.), XXI International Congress of Theoretical and Applied Mechanics, Abstracts and CD-ROM Proceedings. Institute of Fundamental Technological Research, Warsaw, Poland, pp. 1–2.

Zum Gahr, K.-H., Voelker, K., 1999. Friction and wear of SiC fiber-reinforced borosilicate glass mated to steel. Wear 225–229 (Part II), 885–895.